

FUNCTIONAL ANALYSIS OF TWO NOVEL DNA REPAIR FACTORS,
METNASE AND PSO4

Brian Douglas Beck

Submitted to the faculty of the University Graduate School
in partial fulfillment of the requirements
for the degree
Doctor of Philosophy
in the Department of Biochemistry and Molecular Biology
Indiana University

September 2008

Accepted by the Faculty of Indiana University, in partial fulfillment of the requirements for the degree of Doctor of Philosophy.

Suk-Hee Lee, PhD, Chair

D. Wade Clapp, MD

Doctoral Committee

Maureen A. Harrington, PhD

July 28, 2008

Lawrence A. Quilliam, PhD

ACKNOWLEDGEMENTS

I would like to thank Dr. Lee, without whose guidance, patience, and technical training this project could not have been completed. I would also like to thank Sue Lee, whose contributions to the lab have been invaluable.

Others who have assisted me either with experimental assistance or advice include Su-Jung Park, Young Ju Lee, Yaritzabel Roman, Dae-Sik Hah, Byoungsoon Hwang, Jon-Wan Kim, Masahiko Oshige, Joe Dynlacht, John Turchi, Sarah Shuck, Katie Pawelczak, and Samantha Ciccone.

My research committee has also been an excellent source of ideas and suggestions. Thank you to Dr. Quilliam, Dr. Harrington, and Dr. Clapp.

Finally I would like to thank my wife Jessica, and parents Jeff and Sharon Beck for their support and encouragement.

ABSTRACT

Brian Douglas Beck

Functional Analysis of Two Novel DNA Repair Factors, Metnase and Pso4

Metnase is a novel bifunctional protein that contains a SET domain and a transposase domain. Metnase contains sequence-specific DNA binding activity and sequence non-specific DNA cleavage activity, as well as enhances genomic integration of exogenous DNA. Although Metnase can bind specifically to DNA sequences containing a core Terminal Inverted Repeat sequence, this does not explain how the protein could function at sites of DNA damage. Through immunoprecipitation and gel shift assays, I have identified the Pso4 protein as a binding partner of Metnase both *in vitro* and *in vivo*. Pso4 is essential for cell survival in yeast, and cells containing a mutation in Pso4 show increased sensitivity to DNA cross-linking agents. In addition, the protein has sequence-independent DNA binding activity, favoring double-stranded DNA over single-stranded DNA. I demonstrated that the two proteins form a 1:1 stoichiometric complex, and once formed, Metnase can localize to DNA damage foci as shown by knockdown of Pso4 protein using *in vivo* immunofluorescence. In conclusion, this shows that Metnase plays an indispensable role in DNA end joining, possibly through its cleavage activity and association with DNA Ligase IV.

Suk-Hee Lee, PhD, Chair

TABLE OF CONTENTS

List of Figures	vi
Specific Aims	1
Background and Significance	4
Materials and Methods.....	11
Studies	
Aim 1	21
Aim 2	35
Aim 3	45
Aim 4.....	65
Future Directions	86
References.....	88
Curriculum Vitae	

LIST OF FIGURES

Figure 1 – Model of NHEJ in mammalian cells	6
Figure 2 – Schematic diagram of Metnase	9
Figure 3 – Schematic diagram of hPso4	10
Figure 4 – <i>In vitro</i> end joining and <i>E. coli</i> colony formation	23
Figure 5 – Colony formation +/- Metnase	25
Figure 6 – Colony formation using D483A mutant Metnase	27
Figure 7 – Modified Baumann/West <i>in vitro</i> end joining.....	29
Figure 8 – Metnase addition to depleted extracts, end joining <i>in vitro</i>	31
Figure 9 – Model of Metnase function in compatible end DNA end-joining.....	34
Figure 10 – Metnase oligonucleotide cleavage activity.....	36
Figure 11 – Metnase end processing as measured by PCR	38
Figure 12 – Effect of Metnase on compatible and non-compatible ends	39
Figure 13 – wt-Metnase vs D483A cleavage and colony formation	41
Figure 14 – Model of Metnase function in non-compatible DNA end-joining	44
Figure 15 – Nuclear localization of Metnase with Nbs1 following DSB.....	46
Figure 16 – Immunoprecipitation of Metnase binding proteins	47
Figure 17 – Physical association between Metnase and hPso4 on western blot.....	49
Figure 18 – Metnase binds specifically to TIR dsDNA sequences	51
Figure 19 – Stable complex formation on TIR and non-TIR DNA.....	54
Figure 20 – Metnase does not form foci <i>in vivo</i> in the absence of hPso4.....	56
Figure 21 – Transposase domain is not sufficient for Metnase-hPso4 binding	58
Figure 22 – Lack of hPso4 negatively effects inter/intra-molecular end joining	60

Figure 23 – Physical interaction between Metnase molecules <i>in vivo</i>	66
Figure 24 – Glycerol gradient analysis of Metnase	68
Figure 25 – Metnase dimer interaction with dsDNA containing multiple TIRs.....	70
Figure 26 – Metnase has 1:1 stoichiometry with hPso4 on TIR	72
Figure 27 – Titration of Metnase and hPso4 on non-TIR DNA	73
Figure 28 – Stoichiometric analysis of Metnase and/or hPso4 bound to TIR DNA.....	75
Figure 29 – Relative binding activity of Metnase and hPso4, alone or together	76
Figure 30 – Protein interaction negatively influences Metnase-TIR binding.....	78
Figure 31 – Metnase and hPso4 order of addition reaction	80
Figure 32 – Trypsin digestion of Metnase in presence of TIR and non-TIR DNA	81
Figure 33 – Proposed model of Metnase-hPso4 function.....	84

SPECIFIC AIMS

In mammalian cells, DNA double-strand breaks induced by IR and V(D)J recombination are mainly repaired by nonhomologous end-joining (NHEJ) (1-5). The NHEJ repair proteins Ku70/80, DNA PKcs, Artemis, and Xrcc4/ligase IV function both in NHEJ repair and V(D)J recombination repair pathways (2, 3, 5-9). Although these proteins seem sufficient for end joining *in vitro*, recent studies suggest the requirement of additional unknown factors for end joining *in vivo* (2, 6, 10-12). Our lab recently showed that a SET and transposase domain protein, termed Metnase (also known as SETMAR), increases NHEJ repair and mediates genomic integration of exogenous DNA in human 293 cells (13, 14). Metnase possesses two biochemical activities: histone methylation activity at histone 3 lysine 4 and lysine 36 (13) associated with chromatin opening (15-17), and unique DNA cleavage activity (18-20). Our studies identified two Metnase binding partners, DNA ligase IV and hPso4, a human homolog of the *PS04/PRP19* gene that functions in DNA recombination and error-prone repair (21, 22). Based on these findings, I hypothesize that Metnase is required for efficient NHEJ repair in primates. Therefore, the results will likely shed new light on mechanisms of the DSB repair pathway and may lead to new therapeutic possibilities. This study was designed to identify the mechanism by which Metnase and its binding partner(s) improve NHEJ repair. This mechanism was defined by asking four aims as follows:

Aim 1. *In vivo* and *in vitro* analysis of Metnase (SETMAR) Involvement in NHEJ

repair: I used both an *in vitro* end joining assay coupled to *E. coli* colony formation as well as a gel-based inter- and/or intra-molecular end joining assay to examine how Metnase influences joining of compatible and non-compatible ends *in vitro*.

Aim 2. Influence of Metnase DNA cleavage activity on joining of compatible vs.

non-compatible ends: Using an *in vitro* end joining assay I examined how Metnase influences DNA end processing. Cell extracts over-expressing Metnase not only stimulated DNA end joining but also showed an enhanced end processing of non-compatible ends, while the extracts lacking Metnase showed an opposite result.

Importantly, wt-Metnase and not the D483A mutant lacking DNA cleavage activity restores DNA end joining activity *in vivo* and *in vitro*, supporting a role for Metnase DNA cleavage activity in promoting the processing of non-compatible ends, a prerequisite step for the joining of non-compatible ends.

Aim 3. hPso4 is a Metnase binding partners that mediate Metnase function(s) in NHEJ

repair: I showed that hPso4 is a Metnase binding partner that forms a stable complex with Metnase on both TIR and non-TIR DNA. The transposase domain essential for Metnase-TIR interaction is not sufficient for its interaction with non-TIR DNA in the presence of hPso4. I also showed that hPso4 is induced *in vivo* following IR treatment and co-localized with Metnase at DSB sites. Cells treated with hPso4-siRNA failed to show Metnase's localization at DSB sites and Metnase-mediated stimulation of DNA end joining coupled to genomic

integration, suggesting that hPso4 is necessary to bring Metnase to the DSB sites for its function(s) in DNA repair.

Aim 4. *In vitro* analysis of Metnase and/or hPso4 binding to dsDNA: I showed that Metnase exists as a dimer, and forms a 1:1 stoichiometric complex with hPso4 tetramer on dsDNA. Further analysis revealed that hPso4 is solely responsible for binding to DNA once the two proteins form a stable complex, although both Metnase and hPso4 can independently interact with TIR. I also found that Metnase undergoes a conformational change upon binding to DNA, and Metnase bound to TIR is significantly less effective in interacting with hPso4 than free Metnase, suggesting that hPso4, once forming a complex with free Metnase, negatively regulates TIR binding activity of Metnase (transposase), which perhaps is necessary for Metnase localization at non-TIR sites such as DSBs.

BACKGROUND AND SIGNIFICANCE

B.1. End joining of DNA double strand breaks (DSBs) in higher eukaryotes

DSB repair can occur through either NHEJ or homologous recombination (HR), while single-strand annealing is shared between HR and NHEJ (2, 3, 23-25). The error-free pathway of HR restores broken DNA to its original sequence (26-29), whereas the error-prone pathway of NHEJ often processes the DNA by adding or deleting nucleotides before joining the ends (4, 30). However, because HR requires a template chromosome, it is limited to S/G2 phase in most eukaryotes (29), while NHEJ has no such cell cycle limitations (31). Although many of the proteins involved in the two major DSB repair pathways have been identified, the precise mechanisms involved remain poorly understood.

i) NHEJ pathway:

NHEJ repair involves a direct rejoining of the separated DNA ends without the need for a homologous template (32, 33). The repair of DSBs by NHEJ requires the coordinated assembly of damage-responsive proteins at the damage site (2, 3). Upon DSB damage, Ku70/80 complex first binds to the DNA ends (4, 34-38) and recruits DNA-dependent protein kinase catalytic subunit (DNA-PKcs) (39-41), a 465-kDa Serine/Threonine kinase in the phosphoinositol 3-kinase (PI3K) superfamily that mediates bridging of the free ends and then undergoes activation of its kinase (23, 42-44). Kinase activity, particularly phosphorylation at T2609 and S2056 is required for NHEJ (45), but currently its function remains unclear. Artemis associates with DNA-PKcs at the DSB and functions to process

the ends, potentially enhancing homology for re-ligation through a ssDNA-specific 5' → 3' exonuclease (46, 47). Similarly, Mre11 of the MRN complex processes ends through 3' → 5' exonuclease activity (46, 48), as does WRN, a RecQ-like helicase that is phosphorylated by DNA-PKcs and stimulated by Ku complex (49-52). Following exonuclease activity at the free ends, DNA polymerases such as Pol λ and Pol μ are believed to function in filling in of any remaining overhang (53-56). After auto-phosphorylation, DNA-PKcs mediates recruitment of the XRCC4-DNA Ligase IV complex to the DSB site (57-59). The recruitment of the XRCC4-DNA ligase IV complex is essential for the final step of ligation (5, 38, 60, 61). XLF, also known as Cernunnos, is a newly identified core factor of the NHEJ pathway (62-64), and is known to stimulate DNA ligase IV *in vitro* through its interaction with XRCC4 (62, 64, 65).

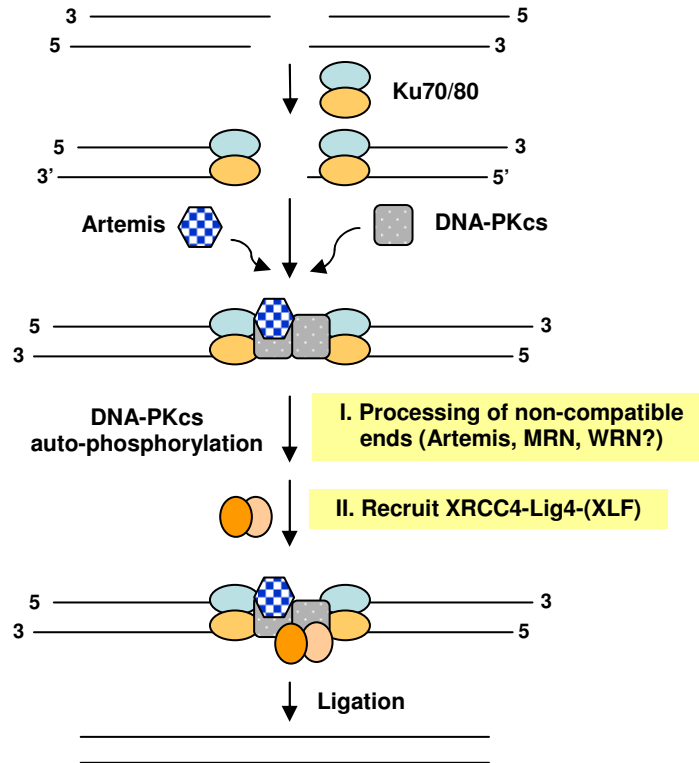


Figure 1. Model of NHEJ in mammalian cells. Non-Homologous End Joining (NHEJ) is the major pathway for DNA repair in mammals due to its cell cycle independence. Briefly, Ku70/80 binds the broken ends and DNA-PKcs moves to the site of damage and is autophosphorylated. After end processing, XRCC4, DNA Ligase IV, and XLF are recruited to the repair complex, and ligation occurs.

ii) Homologous recombination repair (HRR) pathway:

HR-mediated DSB repair is highly conserved through evolution and comprise the primary DSB repair pathway in prokaryotes and lower eukaryotes (24). In the earliest stages of DSB repair by HRR, ataxia-telangiectasia mutated protein (ATM) senses and perhaps binds to the DSB (66-68), and phosphorylates histone H2AX (69, 70), which would then attract breast cancer susceptibility gene 1 (BRCA1) (66, 67) and Nijmegen breakage syndrome protein 1 (Nbs1) (66, 71-73), also phosphorylated by ATM (24). BRCA1 may

help serve as an anchor and coordinator of the repair events that follow (24, 74). BRCA2, attracted to the DSB by BRCA1, facilitates the loading of RAD51 onto RPA-coated DNA overhangs with the help of RAD51 paralogs that in turn attract RAD52 and RAD54 (75, 76), perhaps with the help of DNA helicase(s), the Bloom syndrome protein (BLM) and/or Werner syndrome protein (WRN) (77, 78). BLM and WRN interact with Holliday junctions (79, 80). From this point, there are two possibilities to finish HRR; 1) by non-crossing-over in which case the Holliday junctions disengage and DNA strands pair followed by gap filling (81), or 2) by a crossing-over from Holliday junction resolution and gap-filling (82). It is not known as to which DNA polymerase and ligase are involved in the polymerization and ligation steps.

B.2. Other factors linked to NHEJ repair

i) Metnase:

Metnase, also known as SETMAR, is a 80-kD novel SET [Su(var)3-9, Enhancer-of-zeste, Trithorax]- transposase fusion protein found in anthropoids (83, 84). It possesses histone lysine methyltransferase (HLMT) activity at histone 3 lysine 4 and lysine 36 (13) associated with chromatin opening (15, 17, 85-87) and a transposase domain containing the DDE acidic motif conserved among retroviral integrase and transposase families (Figure 2). It also possesses a sequence-specific DNA binding activity that recognizes a 19-mer core of the 5'-terminal inverted repeats (TIR) of the Hsmar1 element (18, 20, 83). The human chromosomes contain over 7000 sites that are either identical or with a single mismatch to the 19 bp of Metnase binding site (18, 20, 83, 88), suggesting that the human genome contains an enormous reservoir of potential Metnase binding sites. However,

unlike transposases, Metnase does not have any TIR sequences flanking its genetic material, indicating that it is not encoded by a human transposon (13, 84, 89). The Metnase SET domain contains homologies to the two conserved amino-acid sequences in the SET domain of SUV39H1 (NHSCXPN and GEELXXXYY) that are likely responsible for the histone methyltransferase activity (90) (Figure 1). Similar to SUV39H1, Metnase also has a perfect consensus post-SET domain (CXCX₄C).

The discovery of a potential role for Metnase in DNA repair resulted from the finding that Metnase over-expression increased precise and imprecise NHEJ repair *in vivo* (13). Specifically, over-expression of Metnase resulted in approximately a 3-fold increase in both precise and imprecise NHEJ as measured by colony formation following treatment with IR, while knockdown of Metnase expression through Metnase-specific siRNA resulted in a 12-20 fold reduction in NHEJ repair as analyzed by the same methods, providing further evidence of a linkage between Metnase and NHEJ (13, 91). The promotion of DSB repair by the SET domain of Metnase suggests that Metnase may function in opening chromatin, as well as enhancing accessibility of repair factors. In support of this hypothesis, mutating essential amino acid residues in the histone methyltransferase domain of Metnase reduced the ability to stimulate NHEJ repair (13).

Metnase is also involved in genomic integration of foreign DNA (13, 14), and this may also rely on other NHEJ proteins (92-94). Metnase over-expression in human 293 cells increased integration of a Metnase expression vector, and it increased integration of a co-transfected vector (13), suggesting that Metnase promotes genomic integration both

in *cis* and in *trans*. Upon deletion of either the SET or the transposase domain, the ability of the other Metnase domain to promote foreign DNA integration was abrogated, indicating that both domains are required for this function (13). Over-expression of Metnase also promoted integration of retroviral DNA (13, 14). Metnase promotion of the integration of widely varied exogenous DNA sequences integration indicates that this activity is DNA sequence-independent. This distinguishes Metnase from transposases, which act only on transposon-specific sequences.

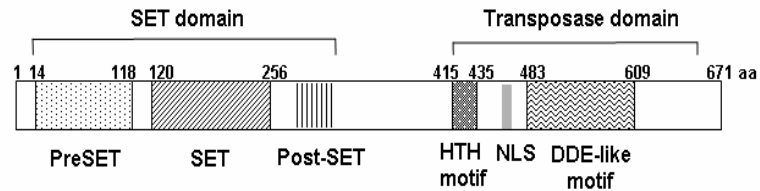


Figure 2. Schematic diagram of Metnase. The PreSET domain contains a cysteine- and histidine-rich putative Zn^{2+} binding motif. The SET domain has the histone lysine methyl transferase motif, and the transposase domain contains helix-turn-helix and DDE-like motifs.

ii) *hPso4*:

hPso4 is a human homolog of the 55-kDa protein encoded by the *PS04/PRP19* gene in *Saccharomyces cerevisiae* that has pleiotropic functions in DNA recombination and error-prone repair (21). *hPso4* contains six successive WD-40 motif at the C-terminus that is known to form a structural interface for the assembly of multiprotein complexes (22, 95), and has been identified as a component of the nuclear matrix (NMP200) (96) (Figure 3). *hPso4* is a part of the pre-mRNA splicing complex consisting of *Pso4*, *Cdc5L*, *Plrg1*, and *Spf27* (97), and has been previously linked to DNA repair through a direct physical

interaction between Cdc5L and WRN, the protein deficient in Werner Syndrome (98). Additionally, Pso4 mutants in *S. cerevisiae* show heightened sensitivity to interstrand crosslink DNA damage (21). Recent studies with hPso4 indicated that it interacts with terminal deoxynucleotidyl transferase (TdT). TdT nucleotides to DNA ends generated during V(D)J recombination that are subsequently processed by proteins involved in general DSB repair pathways (2, 22, 45). Purified hPso4 binds double-stranded DNA in a sequence-nonspecific manner but does not bind single-stranded DNA. hPso4 expression is induced in cells by IR and interstrand crosslinking (22). Loss of hPso4 expression by siRNA results in accumulation of DSBs and decreased cell survival after DNA damage. Taken together these data suggest that hPso4 plays a unique role in mammalian DNA DSB repair. Nonetheless, the specific role(s) for hPso4 in DSB repair is not known.

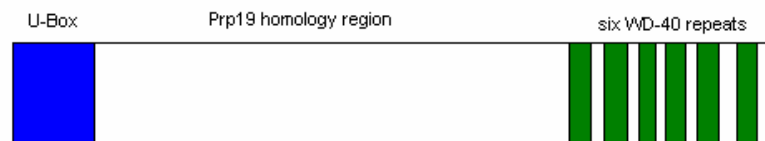


Figure 3. Schematic diagram of hPso4. The U-box domain is involved in ubiquitin ligase activity. The six WD-40 motifs at the C-terminus of the protein act as a site for protein-protein interactions, and possibly as a scaffolding for assembly of protein complexes.

MATERIALS AND METHODS

Cells, Enzymes, and Chemicals

The Human Embryonic Kidney (HEK 293) cell line was grown in Dulbecco's modified Eagle's media (DMEM)-F12 (GIBCO-BRL) supplemented with 10% fetal calf serum (GIBCO-BRL), penicillin (10 units/mL, Sigma), and streptomycin (0.1 mg/mL, Sigma).

Mouse Ku80^{-/-}, DNA-PK^{-/-} and ATM^{-/-} cells were previously described (13, 99).

Restriction enzymes (BamH I, Hind III, Kpn I, EcoR V, and Pst I) were obtained from Promega (Madison, WI). [γ -³²P]-ATP (3000 Ci/mmol) was from Perkin-Elmer and Analytical Science (Boston, MA) and Bradford reagents and protein molecular weight markers were purchased from Bio-Rad (Hercules, CA). The oligonucleotides were obtained from Integrated DNA Technologies (Coralville, IA).

Cis-dichlorodiammineplatinum(II) (CDDP; cisplatin) and anti-FLAG and -V5 monoclonal antibodies were obtained from Sigma (St. Louis, MO) and Invitrogen (Carlsbad, CA) respectively. DE81 filters from Whatman Bio System (Maidstone, England), heparin-Sepharose from Amersham Biosciences (Piscataway, NJ), and Bradford reagents and protein molecular weight markers were purchased from Bio-Rad (Hercules, CA). An anti-Metnase antiserum (polyclonal) was generated from rabbits using two peptides representing amino acids 483-495 (DEKWILYDNRRRS) and 659-671 (WQKCVDCNGSYFD) (13), and an anti-Pso4 polyclonal antibody specific for human Pso4 was obtained from Calbiochem (Gibbstown, NJ). Flag peptide was synthesized from the peptide core facilities at the IU School of Medicine.

Generation of stable cell lines, preparation of cell extracts, and immunoblot analysis

HEK293 cells stably over-expressing wt-Metnase or wt-hPso4 were generated by transfection with a vector harboring FLAG-Metnase, V5-Metnase, or FLAG-hPso4 using FuGENE6 transfection reagent (Roche Molecular Biologicals, Basel, Switzerland). This was followed by selection in G418 (Invitrogen) supplemented media for 14 days, after which a single colony was isolated and amplified. For preparation of cell extracts, cells were briefly washed with phosphate-buffered saline (PBS) and lysed in a buffer containing 25 mM HEPES (pH 7.5), 0.3 M NaCl, 1.5 mM MgCl₂, 0.2 mM EDTA, 0.5% Triton X-100, 20 mM β-glycerolphosphate, 1 mM sodium vanadate, 1 mM DTT, and protease inhibitor cocktails (Sigma). Cell lysates (50 μg) were loaded onto a 10% SDS-PAGE and following gel electrophoresis, proteins were transferred to a PVDF membrane (Millipore, Billerica, MA), immunoblotted with primary antibody followed by peroxidase-coupled secondary antibody (Amersham, Piscataway, NJ) and an enhanced chemi-luminescence (Amersham, Piscataway, NJ) reaction prior to visualization on Kodak-o-mat film (Eastman Kodakm Rochester, NY). Metnase under-expressors were generated by stable transfection of the human 293 cell line by Oligofectamine with either pRNA-U6.1/Hyg (Genescript) for the control or pRNA-U6.1/Hyg-siRNA-Metnase to reduce the expression of endogenous Metnase. Transfectants were selected in hygromycin (150 μg/mL) for 10-14 days. Reverse transcription-PCR was used to initially screen for clones that had a reduced expression of Metnase compared to the control U6 clone. The primers for Metnase and 18S and the sequence for the Metnase siRNA were described previously (13).

Purification of FLAG-Metnase and FLAG-hPso4

Metnase- (or hPso4-) expressing cells (1.6×10^8) were suspended in 20 mL of extraction buffer (TEGDN; 50 mM Tris-HCl pH 7.5, 1 mM EDTA, 10% glycerol, 5 mM DTT, 1.0% Nonidet-P40, and mammalian protease inhibitor cocktails containing 0.2 M NaCl), and centrifuged ($40,000 \times g$) for 3 hours. The supernate was incubated at 4°C for 60 min with anti-FLAG mouse monoclonal antibody (Sigma) that had been pre-equilibrated with TEGDN extraction buffer containing 0.2 M NaCl. The antibody-protein solution was then loaded onto a column containing protein G agarose (2.5 mL). The column was washed with three column volumes of TEGDN-1.5 M NaCl buffer prior to elution of the protein with TEGDN-0.2 M NaCl containing FLAG peptide (500 $\mu\text{g}/\text{mL}$). The elutant was checked for protein concentration using an Ultrospec 2000 spectrophotometer (Pharmacia, Stockholm, Sweden) and positive fractions were combined and dialyzed against 50 mM Tris-Cl pH 7.5, 50 mM NaCl, 100 μM DTT, 0.01% NP-40, and 10% glycerol at 4°C overnight and stored at -80°C.

SDS-PAGE and western blot analysis

Protein fractions were analyzed by 10% SDS-polyacrylamide gel electrophoresis (SDS-PAGE). For visualization, the gel was silver-stained by fixation overnight in 50% methanol, 12% acetic acid, and 500 $\mu\text{L}/\text{L}$ 37% formaldehyde. The gel was dehydrated in 50% ethanol for 20 minutes, then briefly rinsed with sodium thiosulfate (0.2 g/L) for 1 minute to remove any trace silver complexes in the gel. The gel was rinsed three times for 1 minute each, then stained with silver nitrate (0.2 g/L) and 37% formaldehyde (750 $\mu\text{L}/\text{L}$). After three additional rinses in deionized water, the gel was developed using sodium

carbonate (6 g/L), sodium thiosulfate (0.2 g/L), and 37% formaldehyde (500 μ L/L). Staining was stopped with 1% acetic acid. For western blotting, protein was then transferred to polyvinylidene difluoride (PVDF) membrane, probed with an anti-FLAG (monoclonal mouse IgG, Sigma) or an anti-Metnase antibody (polyclonal rabbit IgG) followed by horseradish peroxidase-conjugated secondary antibody. Proteins were visualized using the ECL system (Amersham Biosciences).

Electrophoretic mobility shift assay (EMSA) of protein-DNA interaction

Duplex DNA was labeled with [γ - 32 P]-ATP (3,000 Ci/mmol) and T4 polynucleotide kinase (Roche Molecular Biologicals) according to the manufacturer's instructions. The indicated amount of purified Metnase and/or hPso4 was incubated in a reaction mixture containing 50 mM Tris-Cl pH 7.5, 50 mM NaCl, 1 mM DTT, 0.2 mg/mL BSA, and 5% glycerol for 15 minutes at room temperature. Next, 200 fmol of 5'- 32 P-labeled DNA was added and the reaction incubated at room temperature for 15 min. The Metnase-DNA complex was analyzed on either 5% polyacrylamide gel (acrylamide:bis-acrylamide = 29:1) in 0.5X TBE or 1% vertical agarose gel in 1X TBE. The gels were dried and exposed to x-ray films (Kodak). For quantification, the bands of interest were excised from the gels and measured for radioactivity using a Beckman Scintillation Counter LS 6500. Alternatively, the individual DNA was quantified using the NIH image program (version 1.62).

DNA substrates

DNA substrates were obtained from the Integrated DNA Technologies (Coralville, IA).

The 32-nucleotide dsDNAs containing either the 19-mer core sequence necessary for Metnase binding (TIR32) or 2x5 nucleotide mutation at the core (MAR3M) were

previously described. For Metnase-induced DNA looping experiments, 118 base DNA

oligonucleotides containing either two TIR32 sequences in the forward direction separated

by 54bp of random nucleotides (Fwd-Fwd template: 5'-AGG TTG GTG CAA AAG TAA

TTG CGG AGC TGG CTA TCG GAA CTC TCG GAA GTT GGG TCA GTT ACA ACG

CGC CAC CCG CGC CCC GTA CTG ATA GCA GGG TGC AAA AGT AAT TGC

GGA GGT T-3') or a forward TIR32 sequence and a reverse TIR32 sequence separated by

the same 54-bp nucleotides (Fwd-Rev template: 5'-AGG TTG GTG CAA AAG TAA TTG

CGG AGC TGG CTA TCG GAA CTC TCG GAA GTT GGG TCA GTT ACA ACG CGC

CAC CCG CGC CCC GTA CTG ATA GCA GGG CGT TAA TGA AAA CGT GGA

GGT T-3') were annealed. For Metnase-induced DNA looping experiments, 118 base

DNA oligomers containing either two TIR32 sequences in the forward direction separated

by 54 bp of random nucleotides (Fwd-Fwd template: 5'-AGG TTG GTG CAA AAG TAA

TTG CGG AGC TGG CTA TCG GAA CTC TCG GAA GTT GGG TCA GTT ACA ACG

CGC CAC CCG CGC CCC GTA CTG ATA GCA GGG TGC AAA AGT AAT TGC

GGA GGT T-3') or a forward TIR32 sequence and a reverse TIR32 sequence separated by

the same 54-bp nucleotides (Fwd-Rev template: 5'-AGG TTG GTG CAA AAG TAA TTG

CGG AGC TGG CTA TCG GAA CTC TCG GAA GTT GGG TCA GTT ACA ACG CGC

CAC CCG CGC CCC GTA CTG ATA GCA GGG CGT TAA TGA AAA CGT GGA

GGT T-3') were annealed.

Identification of Metnase-associated proteins

Proteins associated with Metnase were collected by immunoprecipitation with an anti-Flag M2 antibody (Sigma) and Protein G agarose beads (Upstate, Temecula, CA). Whole cell extracts of 10^7 293 cells over-expressing Flag-Metnase were incubated with 3 μ g antibody at 4°C for 2 hrs, followed by addition of 100 μ L Protein G agarose beads overnight. The complex was washed four times with 25 mM Tris-HCl (pH 7.5) containing 250 mM NaCl prior to running on a 10% SDS-PAGE. After staining the gel with Coomassie blue, individual bands were excised and immersed in 100 μ L of 0.1 M ammonium bicarbonate and 50% acetonitrile (by volume) to completely cover the gel pieces. After incubation at 37°C for 30 min, the gel pieces were dehydrated with 100 μ L of acetonitrile for 5 min and rehydrated with 100 μ L of 10 mM DTT at 55°C for 45 min for reduction. Following alkylation with 100 μ L of 55 mM iodoacetamide for 30 min at 37°C, the gel pieces were briefly dehydrated with 100 μ L of acetonitrile and treated with a trypsin solution (Promega V5280, 0.1-0.5 μ g) overnight at 37°C. Following trypsin digestion, peptides were extracted with 0.1% trifluoroacetic acid and injected onto a 75 μ m x 5 cm C-18 reverse-phase column. Peptides were eluted with a gradient from 5-45% acetonitrile over 30 min using an Agilent 1100 series nanopump. The reverse phase column was interfaced with a LTQ ion trap mass spectrometer (Thermo, Waltham, MA), and data were collected in the Data Dependent Neutral Loss MS3 mode. MS/MS spectra were searched against the International Protein Index (IPI) human protein database using a SEQUEST algorithm.

Transfection of cells with siRNA

A control scrambled siRNA, Metnase-specific, and hPso4-specific siRNA were obtained from Dharmacon Research Co. (Lafayette, CO). Human 293 cells (2.0×10^4) were plated on 6-well plates and incubated for 24 hrs prior to transfection. Cells were washed once with fresh medium and siRNA (0.2-0.4 μ M) was diluted in DMEM/F12 to a final volume of 200 μ L. The diluted siRNA samples were combined with Oligofectamine (Invitrogen), and incubated for 20 min at room temperature before adding to cells. After incubation for 4 h, 0.5 mL culture medium containing 30% serum was added without removing the transfection mixture, and cells were further incubated for 48-72 hrs. Cell lysates were prepared and examined for efficacy of siRNA by western blot analysis.

Laser scanning confocal microscopy

Cells were grown to 70% confluence on a sterilized Labtek II coverslip, irradiated with Gammacell-40 exactor (Nordion, Ottawa, Canada) as a ^{137}Cs source, and further incubated at 37°C until harvest. Immunofluorescence microscopy was carried out as described previously (99, 100). Images were collected using a Zeiss LSM-510 confocal microscopy.

DNA end joining coupled to genomic integration analysis

Chromosomal integration was analyzed by the ability of cells to pass on to progeny foreign non-homologous DNA containing a selectable marker. pRNA/U6.Hygro plasmid was transfected into 293 cells stably expressing mock (pFlag2 vector), pFlag2-wtMetnase, or pFlag2-D483A using calcium phosphate transfection method as previously described (101). Forty-eight hours after transfection, varying numbers of cells were plated into 100 mm dishes

and 24 hours later the selection media (hygromycin: 0.15 mg/mL) was added. Cells were incubated for 14 days in the presence of hygromycin. Harvested cells were washed twice with PBS, stained with 0.17% methylene blue in methanol, and colonies defined as greater than 50 cells were counted. All experiments were performed three times in triplicate.

Glycerol gradient sedimentation

Immunoaffinity-purified Metnase or hPso4 proteins were sedimented through a linear 10-35% (vol/vol) glycerol gradient at 45,500 rpm for 26 hrs at 4°C. Fractions (175 µL/each) were collected from the bottom, and the aliquots were run on 10% SDS-PAGE for silver staining and western blot analysis or 5% native gel for dsDNA binding activity.

Preparation of cell extracts

Whole cell extracts were prepared from the human 293 cell line as described previously (102). Briefly, human 293 cells expressing different levels of Metnase were grown in 150 mm dishes. Cells were harvested at ~90% confluency, washed three times in ice-cold PBS and once in hypotonic lysis buffer (10 mM Tris-HCl, pH 8.0, 1 mM EDTA, and 5 mM DTT). Cells were resuspended in 500 µL of hypotonic buffer, incubated on ice for 20 min and homogenized after addition of protease inhibitors (0.17 µg/mL phenylmethyl-sulfonyl fluoride, 1 µg/mL aprotinin, 0.01 units/mL trypsin inhibitor, 1 µg/mL pepstatin, 1 µg/mL chymostatin, 1 µg/mL leupeptin). Following 20 min incubation on ice, 0.5 volume of high-salt buffer (50 mM Tris-HCl, pH 7.5, 1 M KCl, 2 mM EDTA, 2 mM DTT) was added to the cell lysates prior to centrifugation for 3 hr at 42,000 rpm in a Beckman SW55 rotor. The supernates were dialyzed against E buffer (20 mM Tris-HCl pH 8.0, 0.1 M KOAc,

20% glycerol (v/v), 0.5 mM EDTA, 1 mM DTT) for 3 hours, flash-frozen on dry ice, and stored at -80°C.

***In vitro* DNA end joining assay coupled to *E. coli* colony formation**

Reactions mixtures (100 µL) contained 50 mM Tris-HCl (pH 7.5), 0.5 mM Mg-acetate, 60 mM potassium acetate, 2 mM ATP, 1 mM DTT, and 100 µg/mL BSA. Where indicated, dNTPs (2.5 mM) were included in the reaction mixtures. Cell-free extracts were pre-incubated for 5 min at 37°C before addition of 1.0 µg of DNA substrate. Following incubation for 1 hour at 37°C, DNA products were deproteinized, purified by QIAQuick Kit (Qiagen, Valencia, CA), and transformed into high efficiency *E. coli* DH5-alpha competent cells ($> 1.0 \times 10^8$ cfu/µg) for colony formation. Where indicated, PCR amplification of end joining products was performed using Taq DNA polymerase (Promega, Madison, WI) and two primers (M13 Reverse and T7 primers).

A gel-based DNA end joining assay *in vitro* (Baumann and West end joining assay)(102)

Different volumes of reaction mixtures containing 60 µg of whole cell extracts (human 293 cells) and 5' -³²P-pBS DNA (20 ng) were linearized with Kpn I were incubated for 2 hr at 37°C, and DNA products were deproteinized and analyzed by 0.8% vertical agarose gel electrophoresis. Individual end joining products (circular- monomer, dimer, and trimer) were identified by T4 ligase-treated marker DNA.

DNA cleavage assay

For a cleavage assay of supercoiled DNA, reaction mixtures contained 25 mM Tris-HCl (pH 7.5), supercoiled pBluescript II SK+ phagemid DNA (pBS; 100 ng), the indicated amounts of either MgCl₂ (or MnCl₂), 10 mM DTT, and indicated amount of Metnase. The mixtures were incubated at 37°C for 60 min. After incubation, the mixtures were subjected to 1% agarose gel electrophoresis in TBE (Tris-Boric acid-EDTA) buffer following addition of 5 µL of sample loading buffer consisting of 5% sarkosyl, 0.0025% bromophenol blue and 25% glycerol. DNA separated on agarose gel were stained with ethidium bromide, visualized on a UV transilluminator, and analyzed with the NIH image system (version 1.62). For DNA cleavage assay using oligonucleotides, reaction mixtures (20 µL) containing 5'-³²P-dsDNA (200 fmol) were incubated with indicated amounts of Metnase in the presence of 1 mM MgCl₂. After incubation at 37°C for 60 min, reaction mixtures were analyzed by 16% denaturing polyacrylamide gel for DNA cleavage.

STUDIES

AIM 1. *IN VIVO* AND *IN VITRO* ANALYSIS OF METNASE (SETMAR)

INVOLVEMENT IN NHEJ REPAIR

1.1. Metnase's involvement in NHEJ repair (I): From an *in vitro* end joining assay coupled to *E. coli* colony formation

A recent *in vitro* end joining assay developed by Budman and Chu (103, 104) is an intermolecular end joining reaction that was based on qPCR amplification of joined DNA molecules in the presence of cell-free extracts. The end joining assay is dependent on the Ku complex and DNA-PKcs, and is sensitive to wortmannin. Most importantly, it provides a unique tool to measure joining of various compatible and non-compatible ends, which is crucial for understanding of how DNA ends are processed. On the other hand, this method measures end joined products by PCR amplification. Only one of 10 possible end joining products is detected, and it does not reflect all end joining activity occurred in the reactions (103). Intermolecular joining of two selective ends may be affected by relative activity of the nine other possible end joining events in the reaction mixtures.

To evaluate DNA end joining activity quantitatively, I modified an *in vitro* end joining assay originally described by Baumann and West (102). Circular duplex DNA was linearized by restriction endonuclease digestion, then incubated in the presence of dialyzed cell free extract. DNA was isolated from the reaction and transformed into *E. coli*. End-joining was quantified by formation of ampicillin-resistant *E. coli* colonies. (Figure

4A). In this way, not only are all possible end joining products counted, but also identify essential factors for re-ligation. In addition, those factors that may not be crucial for end joining yet affect efficacy or kinetics of DNA end-joining can be determined.

Ampicillin-resistant *E. coli* colonies were proportionally increased with the amount of linearized DNA and the cell extracts, and reached a maximum in the presence of 30 μ g cell extracts (data not shown). I then tested whether our *in vitro* end joining assay coupled to *E. coli* colony formation represents NHEJ repair rather than a simple end joining. Since NHEJ repair is dependent on the presence of DNA-PK, I examined the effect of wortmannin, a specific PI-3 kinase family inhibitor. Colony formation was dependent on ATP and Mg^{+2} , but was completely inhibited in the presence of wortmannin (Figure 4B). Importantly, joining of compatible ends with 5'- and 3'-overhangs, or blunt ends showed similar levels of re-ligation, and were supported by cell extracts prepared from wild-type mouse fibroblast and ATM^{-/-} cells, but not DNA-PKcs^{-/-} or Ku80^{-/-} cells (Figure 4C). This result was in keeping with previous *in vitro* end joining coupled to PCR assays, and suggests that the *in vitro* end joining assay coupled to *E. coli* colony formation represents NHEJ repair rather than a simple end joining. This provides a useful tool for quantitative measurement of intramolecular end joining *in vitro*.

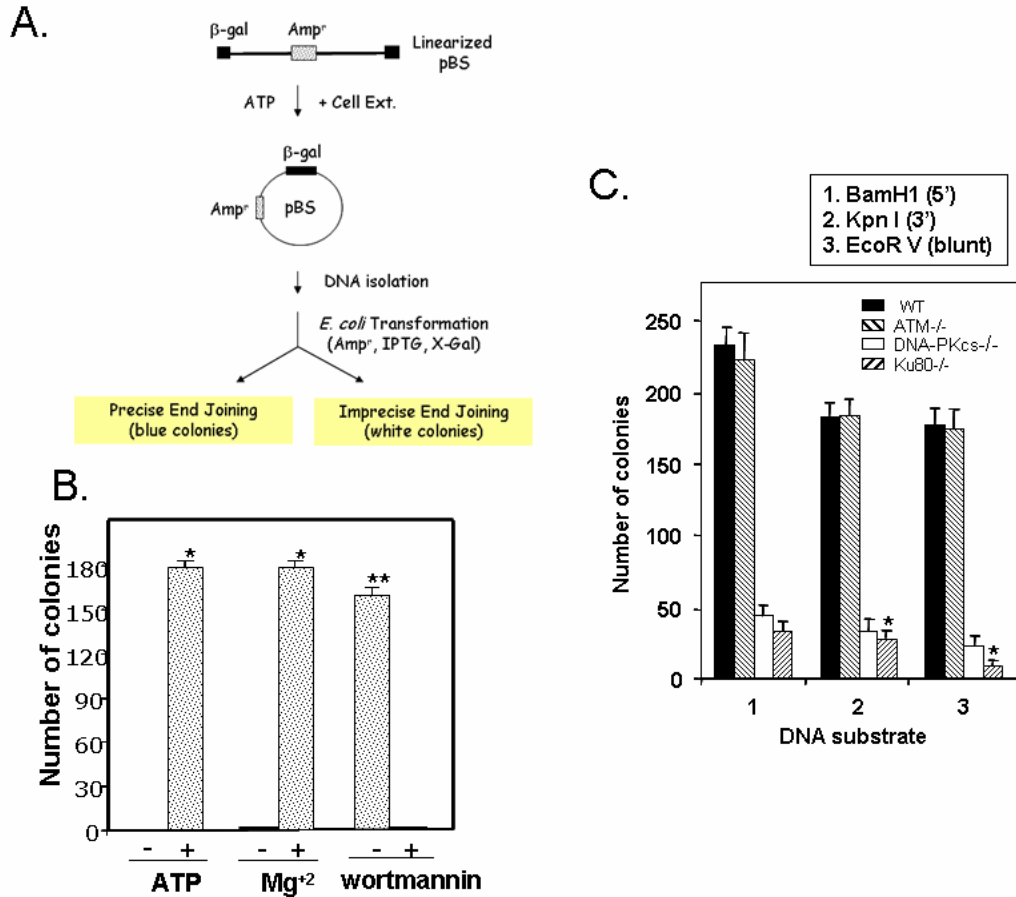


Figure 4. *In vitro* end joining and *E. coli* colony formation. **A)** The assay measured intramolecular end joining of linearized plasmid DNA in the presence of cell extracts. Following DNA isolation, DNA was transformed into *E. coli* for colony counts. **B)** *In vitro* end joining assay is sensitive to wortmannin. *In vitro* end joining assay was carried out in the presence/ absence of 1 mM ATP, 1 mM MgCl₂, or 10 μM wortmannin for 60 min prior to DNA isolation and *E. coli* transformation. The figure is representative of three DNA end joining assays. Values are averages (±SEM) of 6 independent assays. *P < 0.005; **P = 0.01. **C)** *In vitro* end joining assay is dependent on Ku80 and DNA-PKcs. Mouse fibroblast cells lacking Ku80, DNA-PKcs, or ATM were used to prepare cell extracts. The end joining assay coupled to *E. coli* colony formation was carried out in the presence of linearized pBS with 5'-overhangs, 3'-overhangs, or blunt ends. Values are averages (±SEM) of 3 distinct determinations. P < 0.01; *P = 0.05.

1.2. Cell extracts lacking Metnase failed to support the joining of both compatible and non-compatible ends

Metnase promotes NHEJ repair and mediates genomic integration of exogenous DNA in human 293 cells. I therefore examined whether Metnase influences DNA end joining *in vitro*. HEK293 cells were transfected with a V5-tagged pcDNA5.1 plasmid containing a Metnase cDNA, and then were selected with media supplemented with G418 to isolate colonies of cells that stably expressed the plasmid. G418 resistant cells were amplified and whole cell extracts collected. HEK293 cells were transiently transfected with Metnase siRNA for 48 hours and whole cell extracts collected. Western blot comparing wild-type HEK293 cells, with both Metnase under- and over-expressor extracts are seen in Figure 5A. Compared to control 293 cell extracts, extracts from cells over-expressing Metnase showed a 1.25-1.3 fold increase in DNA end joining activity, while those prepared from cells transfected with siRNA-Met showed 8-20 fold reduction in the joining of compatible ends (Figure 5B). A similar result was obtained when joining activity of various non-compatible ends was measured (Figure 5C). This finding is in keeping with our previous *in vivo* finding that Metnase is involved in DNA end joining repair. It also validates that the *in vitro* end joining assay coupled to *E. coli* colony formation as a valuable tool to explore the role(s) for Metnase and other repair factor(s).

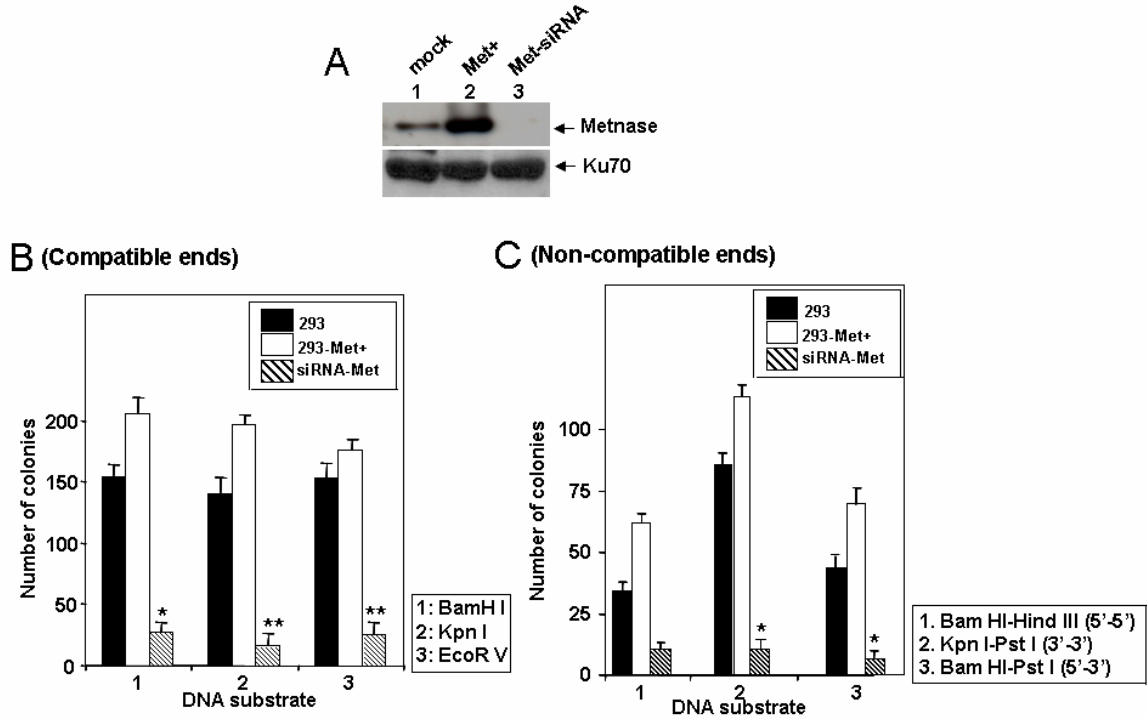
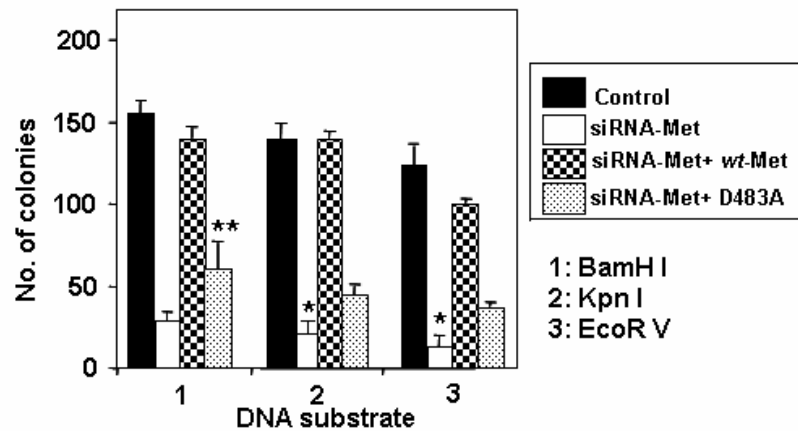


Figure 5. Colony formation +/- Metnase. Cell extracts lacking Metnase failed to support joining of both compatible and non-compatible ends. **A)** Effect of Metnase-siRNA on Metnase expression. Wild-type Human 293 cells (lane 1) were overexpressed with V5-Metnase (lane 2) or treated with Metnase-specific siRNA (lane 3). After 48 hrs, cell extracts were analyzed for Metnase expression by western blot using an anti-V5 antibody. Expression of Ku70 was included as a loading control. **B)** Cell extracts lacking Metnase failed to support the joining of compatible ends *in vitro*. Cell extracts (30 μ g) prepared from 293 cells expressing different level of Metnase (293 cells, *filled bar*; Metnase over-expressor, *open bar*; Metnase-siRNA, *striped bar*) were incubated for 60 min with linearized pBS DNA (1.0 μ g) in the presence of 1 mM MgCl₂ and 1 mM ATP. Following incubation, DNA was isolated and transformed into *E. coli* for colony counts. Numbers 1-3 represent DNA substrates with different ends indicated on the right side of the figure. The figure is representative of three DNA end joining assays. Values are averages (\pm SEM) of 3 distinct determinations. $P < 0.01$; * $P = 0.05$; ** $P = 0.08$. **C)** Cell extracts lacking Metnase failed to support the joining of non-compatible ends *in vitro*. Experiments were done as in panel B, except for the use of linearized pBS with non-compatible ends (1.0 μ g). Numbers 1-3 represent DNA substrates with different ends as indicated on the right. Values are averages (\pm SEM) of 5 distinct determinations. $P < 0.01$; * $P = 0.05$.

1.3. Addition of wt-Metnase and not D483A lacking DNA cleavage activity restored end joining activity of cell extracts lacking Metnase

To see whether poor end joining activity associated with cell extracts prepared from siRNA:Metnase-treated cells was due to a lack of Metnase, I carried out an add-back experiment. Purified wt-Metnase was added to the cell extracts for restoration of end joining activity. Addition of wt-Metnase to cell extracts (prepared from siRNA:Metnase-treated cells) effectively restored joining of both compatible and non-compatible ends. The Metnase D483A mutant lacking DNA cleavage activity partially restored joining of compatible but not non-compatible ends (Figure 6A and 6B). This result suggests that Metnase's DNA cleavage activity may be necessary for joining of non-compatible ends, whereas the interaction of Metnase with DNA Ligase IV may be necessary for joining of compatible ends (14).

A (Compatible ends)



B (Non-compatible ends)

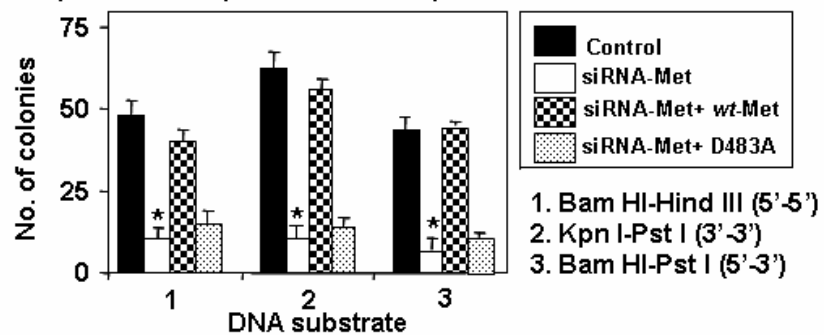


Figure 6. Colony formation using D483A mutant Metnase. Addition of wt-Metnase and not D483A restored DNA end joining activity with cell extracts lacking Metnase. For an *in vitro* end joining assay, cell extracts were prepared from human 293 cells (control) or 293 cells treated with siRNA-Met. Where indicated, 0.2 μ g of purified mammalian wt-Met [siRNA (Met) + wt-Met] or D483A [siRNA(Met) + D483A] was added to the extracts prepared from Met siRNA-treated cells prior to end joining reactions. Reaction mixtures (100 μ L) containing 30 μ g of cell extracts, linearized pBS DNA (1.0 μ g), 1 mM MgCl₂ and 1 mM ATP were incubated for 60 min, and DNA was isolated for transformation into *E. coli* for colony counts. Numbers 1-3 represent DNA substrates with different compatible ends (panel A) or non-compatible ends (panel B) indicated on the right side of the figure. The figure is representative of three DNA end joining assays. Values are averages (\pm SEM) of 3 separate experiments (panel A, $P < 0.01$, * $P = 0.05$, ** $P = 0.08$; panel B, $P < 0.01$, * $P = 0.05$).

1.4. Involvement of Metnase in NHEJ repair (II): The Baumann-West' *in vitro* end joining assay

To further understand Metnase's involvement in NHEJ, the modified Baumann-West end joining assays were carried out in the presence of cell free extracts and 5'-³²P-labeled linearized pBS plasmid DNA. Intra-molecular DNA end-joining products (monomer-circular) were preferentially formed when DNA and protein concentrations were low (30 μ L reaction volume), while inter-molecular joining (dimer and trimer) was favored by higher DNA and protein concentrations (Figure 7A, lanes 2 vs. 3-5). A faster migration of the monomer-circular DNA was likely due to a formation of minichromosomes constructed by reconstituting complexes of core histones in the cell extracts with the pBS DNA. Formation of end joining products was ATP-dependent and wortmannin-sensitive (Figure 7B). In keeping with the intra-molecular end joining assay (Figure 5B), the modified Baumann-West end joining assay showed that cell extracts under-expressing Metnase, compared to control cell extracts, poorly supported joining of compatible ends (Figure 7C).

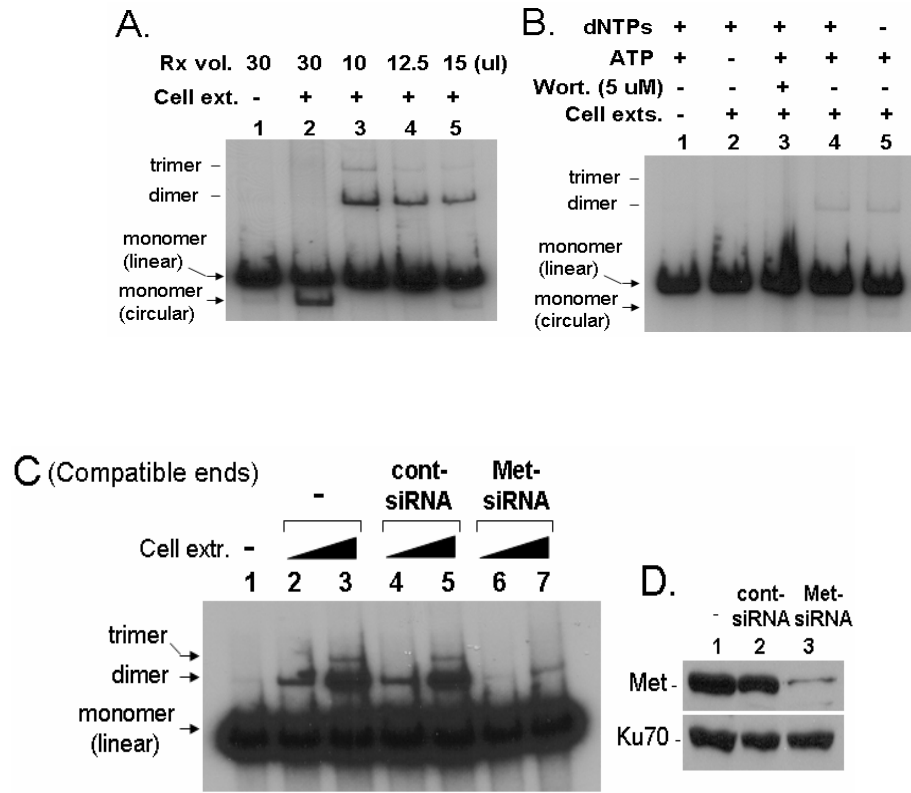


Figure 7. Modified Baumann/West *in vitro* end joining. Cell extracts lacking Metnase poorly supported the joining of compatible ends with the modified Baumann-West end joining assay. **A)** Inter- and intra-molecular end joining with cell-free extracts. Different volumes of reaction mixtures containing 60 μ g of whole cell extracts (human 293 cells) and 20 ng of 5'-³²P-pBS DNA linearized with Kpn I were incubated for 2 hr at 37°C, and DNA products were deproteinized and analyzed by 0.8% vertical agarose gel electrophoresis. Individual end joining products (circular- monomer, dimer, and trimer) were identified by T4 ligase-treated marker DNA. **B)** Reactions performed in 10 μ L total volume with 60 μ g extract and where indicated, 5 uM of wortmannin, 2 mM ATP, or 100 uM of dNTPs was included. **C)** Cell extracts lacking Metnase failed to support joining of compatible ends with a gel-based end joining assay. Reaction mixtures (10 μ L) were the same as Panel A, except the use of two concentrations (30 and 60 μ g) of cell extracts. **D)** Relative amount of Metnase expression in 293 cell extracts (lane 1), extracts from cells harboring siRNA-control-vector (lane 2), and extracts from Met siRNA treated cells (lane 3).

1.5. Addition of wt-Metnase to cell extracts lacking Metnase restored DNA end joining activity

Addition of wt-Metnase (0.01 μ g) to extracts lacking Metnase significantly increased end joining activity (Figure 8A, lanes 6-7 vs. 8-9; Figure 8B, lanes 7 vs. 8-10), whereas it had little or no effect on DNA end joining with control cell extracts (Figure 8A, lanes 2-3 vs. 4-5; Figure 8B, lanes 3 vs. 4-6). This result strongly indicated that a poor end joining activity associated with siRNA:Met-treated cell extracts was due to a lack of Metnase. In a separate approach, I examined how immunodepletion of Metnase from cell extracts affects DNA end joining. Endogenous Metnase was successfully depleted from cell extracts as determined by immunoblot analysis (Figure 7D).

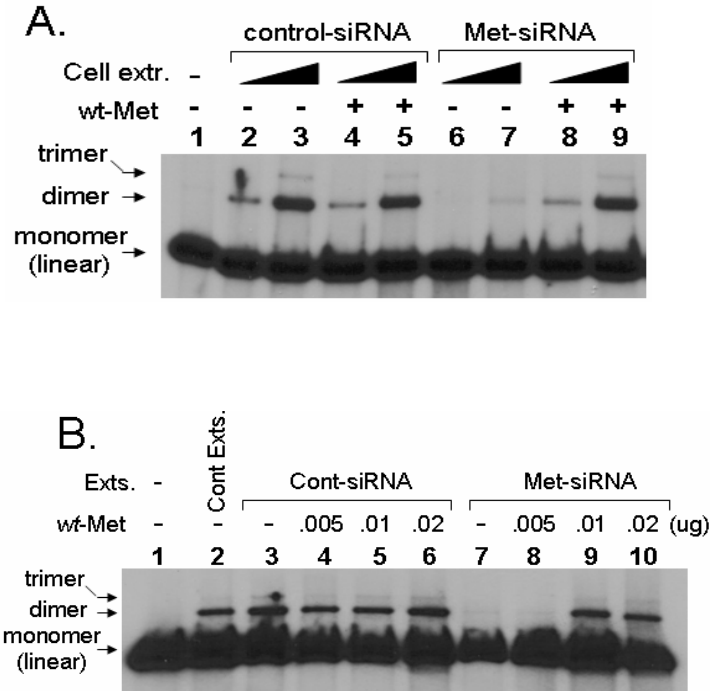


Figure 8. Metnase addition to depleted extracts, end joining *in vitro*. Addition of wt-Metnase to cell extracts lacking Metnase restored DNA end joining activity. **A)** Increasing amounts (30 and 60 μg) of control extracts (control-siRNA) or extracts lacking Metnase (Met-siRNA) were incubated with 20 ng of 5'- ^{32}P -pBS DNA linearized with Kpn I for 2 hr at 37°C. Where indicated, 0.01 μg of wt-Metnase was included. DNA products were analyzed by 0.8% agarose gel electrophoresis. **B)** HEK293 cell extracts (30 μg) (control Ext., Cont-siRNA, and Met-siRNA) were incubated with Kpn I-linearized 5'- ^{32}P -pBS DNA (20 ng) in the presence of increasing amounts of wt-Metnase. End joining products (dimer and trimer) were indicated with arrows.

Discussion:

Non-homologous end joining (NHEJ) is the major DNA repair pathway in mammalian cells, and involves a rapid, if error-prone, rejoining of the two separated DNA ends (2, 3, 23, 24). In addition, the pathway functions in processing cell-directed DSBs in V(D)J recombination in order to create immunological diversity (99, 105-108). Unlike homologous recombination, NHEJ does not require complementary bases at the free DNA ends. Earlier cell-free end joining systems identified the Ku70/80 heterodimer, DNA-PKcs, XRCC4/Ligase4, and end-processing proteins such as Artemis or the MRN complex as required for NHEJ repair *in vitro* (23, 34, 35, 42-44, 48, 53-57). Given that DNA end joining requires processing of non-compatible ends, however, additional factor(s) are necessary for completion of NHEJ in a cell-free system.

The Budman and Chu assay is an *in vitro* intermolecular end joining assay based on PCR amplification of joined REF DNA molecules in the presence of cell-free extracts (6, 7). While this assay allows for compatible and non-compatible end joining products, it explains only one of 10 possible end joining products and may not represent overall end joining events occurring in the reactions. The *in vitro* end joining assay described here is a modified version of an intramolecular joining of linear plasmid DNA (102), which couples end joining products to *E. coli* colony formation for quantitative measurement. In addition, the colony counts were proportional to the amount of cell extract and linearized DNA used, thus experimental results are quantitative. Finally, the assay is Ku70/80 and DNA-PKcs dependent, and results in ligation of both compatible and non-compatible ends, key features of NHEJ. Therefore, the Budman and Chu systems is a good model of *in vivo*

NHEJ systems. The major modification to the assay is that while Baumann and West performed their reactions in a total volume of 20 μL , which tends to favor intermolecular dimerization rather than intramolecular re-circularization. To maximize colony formation, it was essential to produce as many intact circular plasmids as possible, so the reaction volume was increased five-fold to 100 μL , which favored intramolecular end joining. Previous work by our lab has shown that Metnase plays a specific but unknown role in NHEJ and genomic integration of foreign DNA (13, 20). Metnase-mediated stimulation of NHEJ repair *in vivo* requires both SET and transposase domains, suggesting that Metnase's HLMT activity is also involved in NHEJ (13). I have established that thousands of potential Metnase binding sites exist in the genome, and a number of these are in the vicinity of nearby genes encoding DNA repair factors. Perhaps Metnase expression or lack thereof could result in a modification of expression levels of these proteins. The advantage of our modified *in vitro* end joining assay is the results focus on the role of Metnase itself in end joining, and not whether it modifies the expression of additional proteins. Metnase knockdown with siRNA has a significant effect on the ability of cell extracts to enable linearized pBS' to dimerize (Figure 8A and 8B). Because the ability of the cell-free system to restore dimerization is returned upon introduction of exogenous Metnase, I can conclude that Metnase itself has a role in the process other than modulation of expression levels of other proteins (Figure 9). Furthermore, since re-introduction of the Metnase D483A cleavage mutant did not affect end joining levels, this suggests that Metnase cleavage activity plays a major functional role in DNA end joining, perhaps specifically end processing.

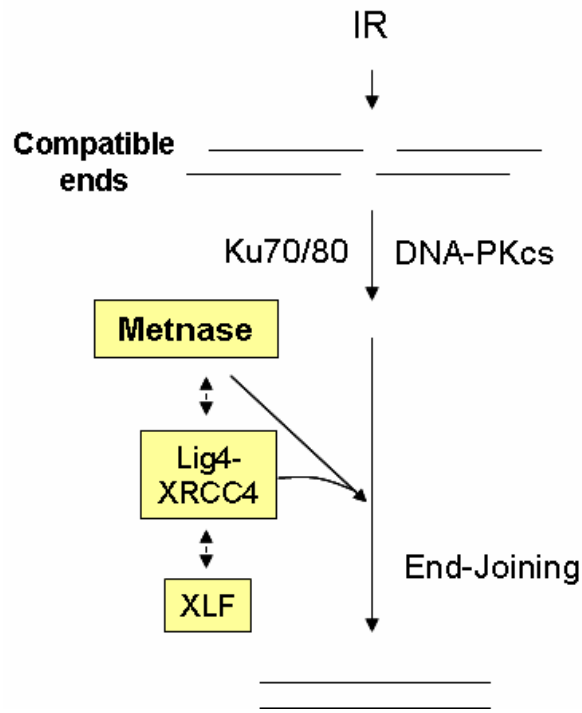


Figure 9. Model of Metnase function in compatible end DNA end-joining. In this model, NHEJ begins in the same way as in Figure 1, with Ku70/80 and DNA-PKcs binding. Experiments showing re-introduction of purified Metnase into cell extracts lacking the protein showed restoration of compatible end DNA end-joining. This may be due to the interaction between Metnase and DNA Ligase IV *in vivo*.

AIM 2. INFLUENCE OF METNASE DNA CLEAVAGE ACTIVITY ON JOINING OF COMPATIBLE VS. NON-COMPATIBLE ENDS

2.1. Metnase has a preferred singlestranded- and singlestranded-overhang DNA cleavage activity

Although the mechanism by which Metnase enhances NHEJ is still not clear, the transposase domain possesses DNA cleavage that may link it to a role in DSB repair. Metnase possesses a unique nuclease activity that mediates cleavage of duplex DNA in the absence of a TIR sequence (20). Arginine 432 within the HTH motif is critical for sequence-specific recognition, but is not required for its DNA cleavage activity. The DDE-like motif, on the other hand, is crucial for Metnase DNA cleavage action. A point mutation in the DDE motif (D483A) abolished Metnase's DNA cleavage activity. This suggests that Metnase's DNA cleavage activity, unlike that of other eukaryotic transposases, is not coupled to its sequence-specific DNA binding. Since a mutant lacking DNA cleavage activity (D483A) failed to support joining of non-compatible ends (Figure 5), I examined whether Metnase has DNA processing activity. First, I compared ssDNA with dsDNA for Metnase's DNA cleavage activity (Figure 10A). Metnase exhibited a significantly higher DNA cleavage activity with ssDNA over dsDNA (Figure 10A, lanes 2-4 vs. 6-8). A kinetic analysis with partial-duplex DNA further demonstrated that Metnase has a DNA cleavage activity preference for ssDNA overhangs (Figure 10B and 10C). Together, these data support a role for Metnase in DNA end processing.

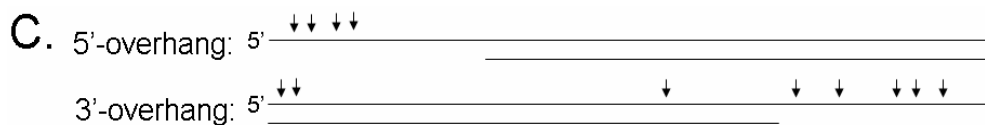
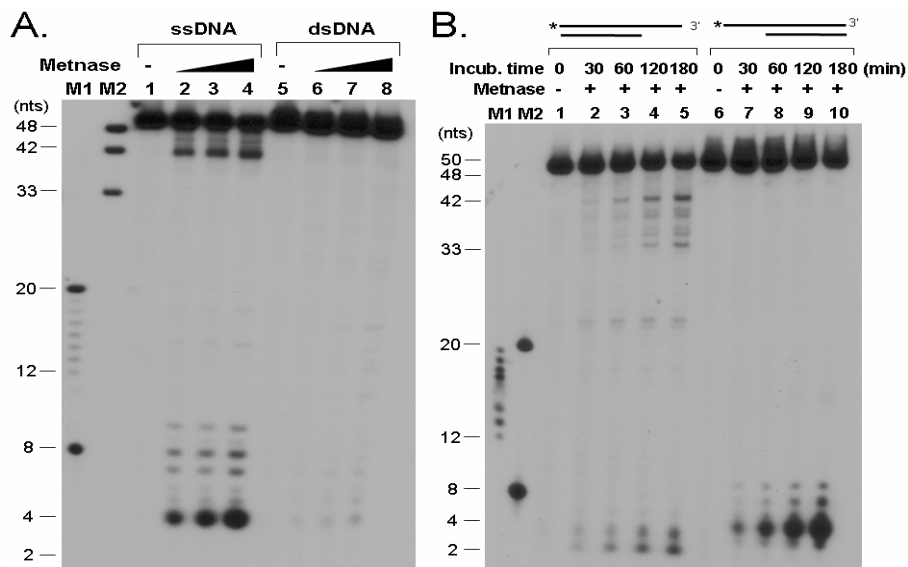


Figure 10. Metnase oligonucleotide cleavage activity. Metnase possesses a preferred DNA cleavage activity with ss- and ss-overhang DNA. **A)** Reaction mixtures (20 μ L) containing 50 fmol of 5'- 32 P-labeled 50-mer ssDNA (lanes 1-4) and 50-mer dsDNA (lanes 5-8) were incubated with 0 (lanes 1 and 5), 0.05 μ g (lanes 2 and 6), 0.1 μ g (lanes 3 and 7), and 0.2 μ g (lanes 4 and 8) of wt-Metnase in the presence of 2 mM $MgCl_2$. After incubation at 37°C for 120 min, reaction mixtures were analyzed by 18% PAGE (8M urea) for DNA cleavage. DNA size markers indicated on the left. **B)** Kinetic analysis of Metnase's DNA cleavage activity with partial duplex DNA (3'- and 5'-overhangs). M1 and M2 represent two DNA markers used in this study. **C)** DNA cleavage sites from Panel B mapped with arrows.

2.2. Involvement of Metnase in the processing of non-compatible ends during end joining *in vitro*

To examine the role for Metnase's DNA cleavage activity in DNA end joining, I further analyzed DNA joining products for non-compatible end processing. Eighteen samples from the joining of three separate non-compatible ends [Kpn I-Pst I (3'-3'), Bam HI-Hind III (5'-5'), and Bam HI-Pst I (3'-5') overhangs] were analyzed in the presence of cell-free extracts generated from cells expressing different levels of Metnase. To assess end processing activity, plasmid DNA isolated from individual colonies was amplified by PCR using T7 and M13 reverse primers. PCR products were then analyzed by 5% PAGE for end processing. A control DNA without any end processing (Figure 11, lane C) produced 210 nucleotides (nts) of PCR product, while end joining of non-compatible ends showed up to 85 nts of base-pair loss following incubation with cell extracts (Figure 11). A vast majority of end joining products showed base-pair loss of up to 10 nts following incubation with cell extracts lacking Metnase (Figures 11C and 12), whereas up to 85 nts of base-pair loss was observed in DNA end joining reactions performed with cell extracts generated from cells over-expressing Metnase (Figure 11B and 12). Cell extracts prepared from control 293 cells showed DNA end processing activity between the Metnase over-expressor and the under-expressor. Together, these results suggest that Metnase's role in the processing of non-compatible ends likely promotes DNA end joining in a cell-free extract system.

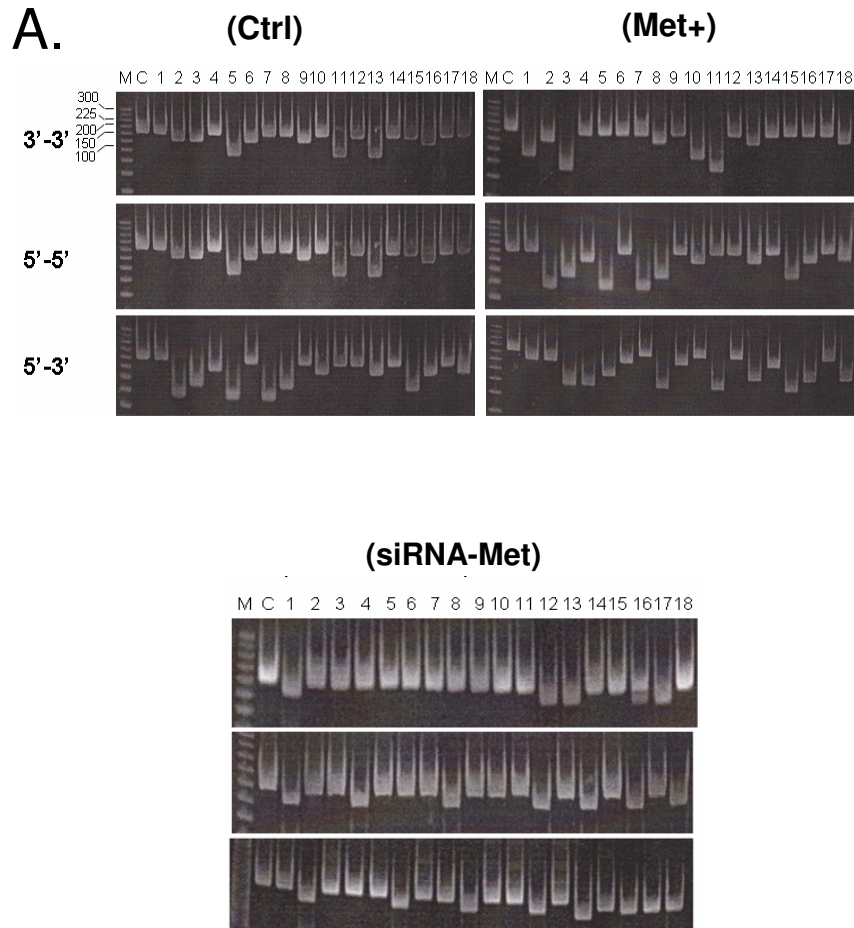


Figure 11. Metnase end processing as measured by PCR. Thirty μg of cell extracts containing different levels of Metnase [(293 cells (Ctrl; **A**), Metnase over-expressor (Met+; **B**), and Metnase-siRNA (siRNA-Met; **C**)] were incubated for 60 min with 1.0 μg of linearized pBS DNA in the presence of 1 mM MgCl_2 and 1 mM ATP. Three linearized DNA with non-compatible ends [3'-3' (Kpn I-Pst I), 5'-5' (Bam HI-Hind III), and 5'-3' (Bam HI-Pst I)] were used for the experiment. End joining products were transformed into *E. coli* and, 18 colonies were picked from each group and analyzed for base-pair loss following PCR amplification of isolated plasmid using T7 primer and M13 reverse primer. M and C represent 25 bp DNA Step Ladder marker and the control 210 bps of PCR product without DNA end processing, respectively.

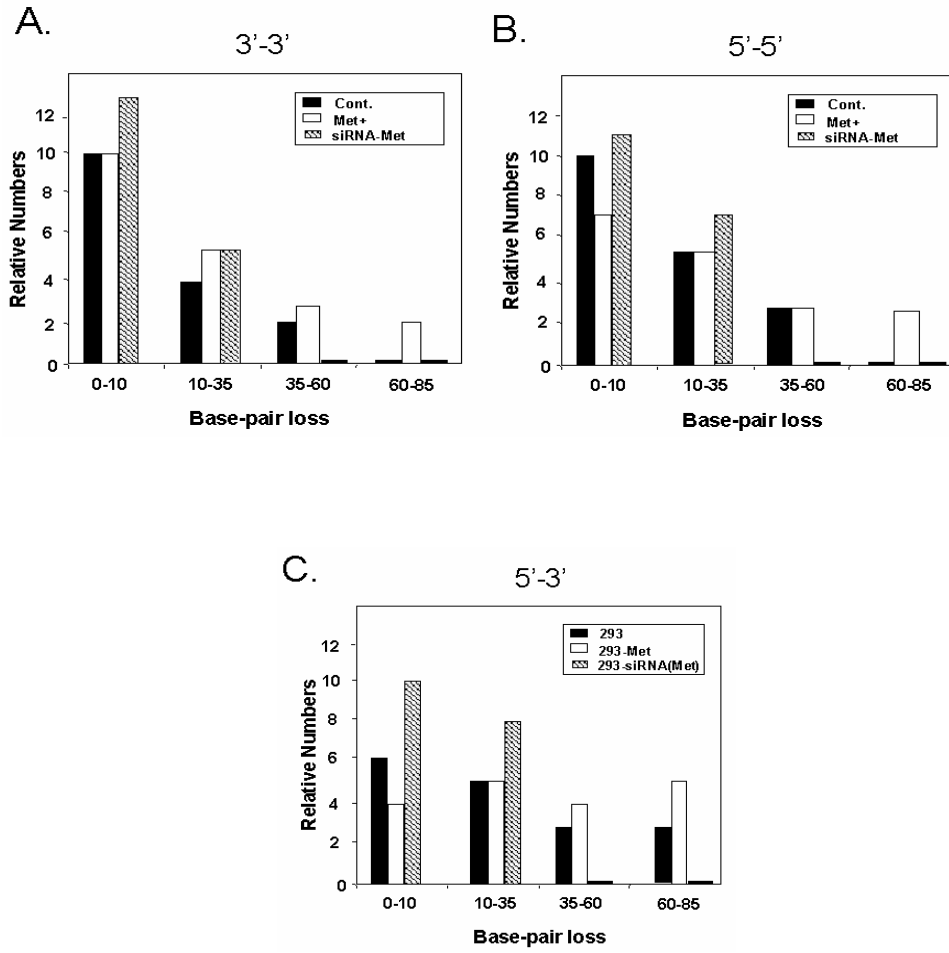


Figure 12. Effect of Metnase on compatible and non-compatible ends. Base-pair loss of end joining products in each group was calculated from Figure 9.

2.3. A mutant lacking DNA cleavage activity (D483A) failed to support Metnase's function in end joining repair *in vivo*

Metnase promotes *in vivo* end joining activity and mediates genomic integration of foreign DNA. A point mutation in the key DDE-like motif (D483A) not only abolishes Metnase's dsDNA cleavage activity (20), but also destroyed its ssDNA cleavage activity (Figure 13D). To address biological relevance of Metnase's DNA cleavage activity, I tested whether over-expression of the D483A Metnase mutant lacking DNA cleavage activity promotes end joining activity *in vivo*. *In vivo* end joining was examined by testing the ability of Metnase to precisely or imprecisely rejoin a plasmid DNA that was linearized within the β -galactosidase gene. Over-expression of wildtype-Metnase (wt-Metnase) increased precise and imprecise end joining by 2.3- and 3.2-fold, respectively; cells over-expressing D483A had little effect on end joining activity (Figure 13B). It was next examined whether the Metnase D483A mutant would stimulate genomic integration of exogenous DNA as measured by the assimilation and passage to progeny of a selective hygromycin-resistance marker. Stable over-expression of wt-Metnase in HEK293 cells did not affect plating efficiency (data not shown). It did however increase integration of a plasmid DNA carrying hygromycin by 4-5-fold. Stable over-expression of Metnase D483A had no effect on genomic integration (Figure 13C). Together, these data suggest that Metnase's DNA cleavage activity is crucial for its function in end joining and genomic integration.

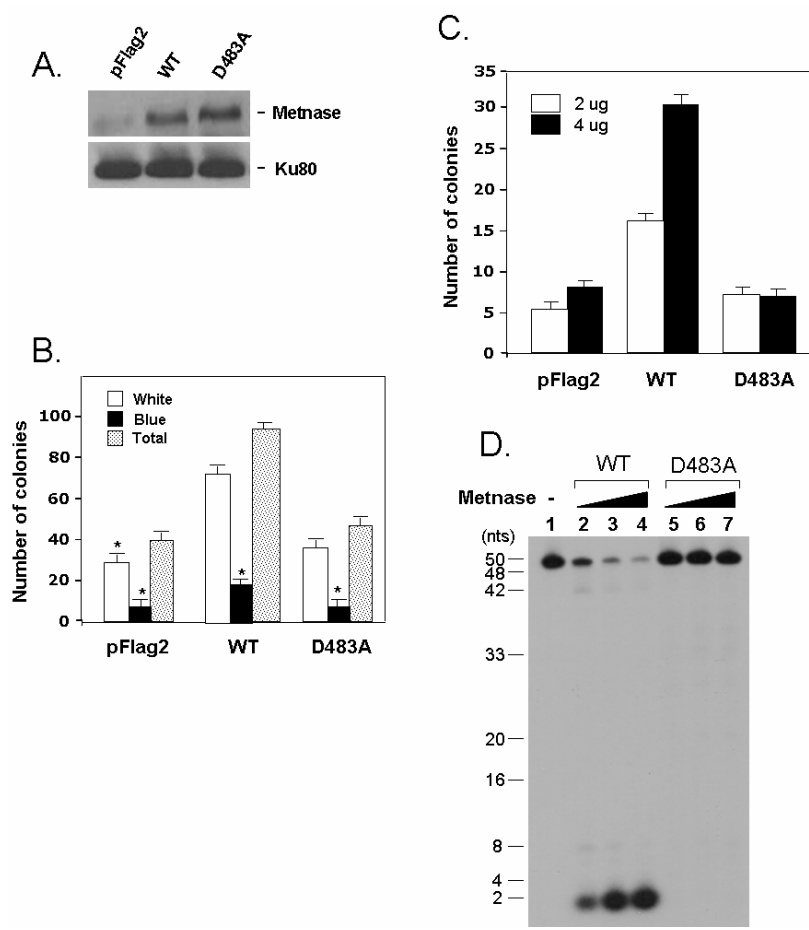


Figure 13. Wt-Metnase vs D483A cleavage and colony formation. **A)** Western blot analysis of 293 cells over-expressing wt-Met (WT) or D483A mutant using an anti-Metnase antibody (top). Ku80 (bottom) was used as an internal control. **B)** Effect of wt-Met and D483A on intra-molecular end joining of *Eco* RI-digested pBS. Stable expression of either wt-Met or D483A in 293 cells was examined for their imprecise repair (white), precise repair (blue), and total NHEJ repair (blue and white colonies). Values are averages (\pm SEM) of 3 distinct determinations. $P < 0.01$; $*P = 0.05$. **C)** Effect of D483A mutation on Metnase-mediated promotion of foreign DNA integration. Human 293 cells stably transfected with pFLAG2, pFLAG2-wt-Met, or pFLAG2-D483A were transfected with increasing concentrations (2 and 4 μ g) of pRNA/U6-Hygro, and the number of hygromycin-resistant colonies was a measure of genomic integration. **D)** Reaction mixtures (20 μ L) containing 50 fmol of 5'- 32 P-labeled 50-mer ssDNA were incubated with 0 (lane 1), 0.05 μ g (lanes 2 and 5), 0.1 μ g (lanes 3 and 6), and 0.2 μ g (lanes 4 and 7) of wt-Metnase (lanes 2-4) or D483A (lanes 5-7) in the presence of 2 mM $MgCl_2$. After incubation at 37°C for 120 min, reaction mixtures were analyzed by 18% PAGE (8M urea) for DNA cleavage. DNA size markers indicated on the left.

Discussion:

The Mre11/Rad50/Nbs1 (MRN) complex and Artemis possess 3'-5' exonuclease and endonuclease activity and ssDNA-specific 5'-3' exonuclease, respectively (46-48). The exonuclease activity of the MRN complex functions in processing mismatched DNA ends prior to ligation, while its endonuclease serves to open hairpin DNA in V(D)J recombination (109). Artemis functions in end-processing and upon phosphorylation by DNA-PKcs, functions in V(D)J hairpin opening (110, 111). Like MRN, Werner Syndrome protein (WRN) also has 3'→5' exonuclease activity (49-52). The exonuclease activity of WRN, a member of the ReqQ-like DNA helicase family, is stimulated by Ku protein, but appears to be negatively regulated by DNA-PKcs. Our *in vitro* work suggests that Metnase also belongs to this group of proteins functioning in the non-homologous end joining pathway. Extracts from cells overexpressing Metnase protein showed increased base pair loss during processing of overhanging DNA ends as compared to extracts containing endogenous levels of Metnase. This result suggests a positive function of Metnase cleavage activity in end processing (Figure 9 and 10). Furthermore, extracts from cells containing diminished amounts of Metnase produced even less base pair loss than extracts containing wild-type Metnase. Thus, the more Metnase protein available in the cell extract, the more extensively end processing occurs. This result was further supported by data showing that extracts from cells overexpressing the Metnase cleavage mutant (D483A) Metnase resulted in similar numbers of *E. coli* colonies (produced from re-ligated linearized pBS' plasmid) as extracts from cells containing only endogenous Metnase. Extracts from cells overexpressing Metnase showed a 2-4 fold increase in colony formation (Figure 11). DNA end-processing may be necessary for re-ligation even in the

presence of compatible ends. Alternatively, DNA end-processing may enhance the existing ability of the cell to re-ligate DSBs by increasing a chance for partial annealing between two non-compatible ends.

This data suggests a role for Metnase in processing of free DNA ends in NHEJ, a reasonable hypothesis regarding end-joining of non-compatible ends. However, it does not explain why overexpressed wild-type Metnase enhances re-ligation of compatible ends while overexpression of the D483A Metnase does not (Figure 6A and 13). Perhaps a currently unrecognized structural alteration exists in the D483A Metnase mutant that interferes with its' association with DNA Ligase IV. Similar to the extracts from cells lacking DNA-PKcs or Ku80 (Figure 4C), the extracts prepared from Metnase-siRNA treated cells failed to support the joining of compatible ends (Figure 5B). These data suggest that Metnase has a separate role in the joining of compatible ends, perhaps by interacting with other NHEJ repair factor(s). DNA processing activity also contributes to the immunological diversity generated by V(D)J recombination. It remains to be seen whether Metnase and its DNA cleavage activity also plays a role in V(D)J recombination.

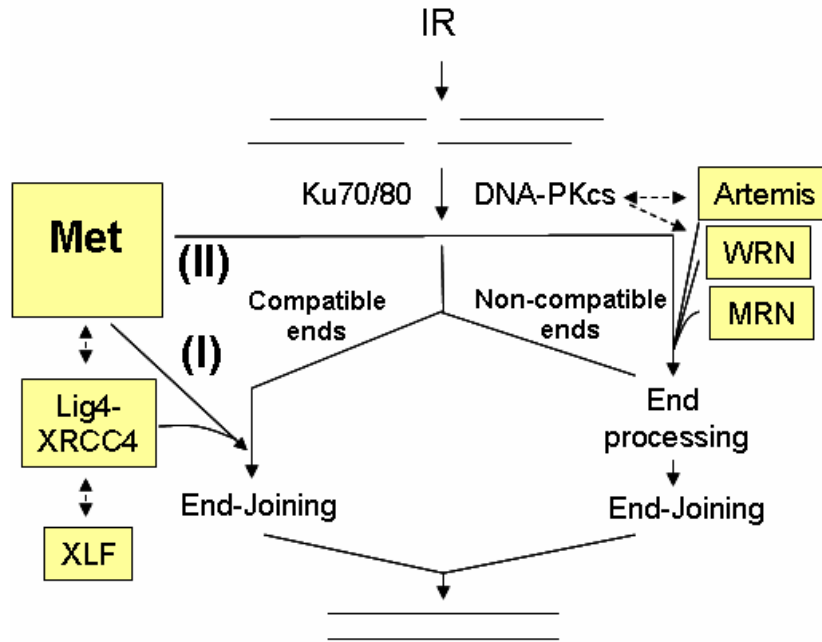


Figure 14. Metnase function in non-compatible DNA end-joining. This data has demonstrated that Metnase has a role in both compatible and non-compatible end-joining. In this model, Metnase contributes to compatible end joining through association with DNA Ligase IV, and to non-compatible end joining through processing of non-homologous overhang DNA.

AIM 3. HPSO4 IS A METNASE BINDING PARTNER THAT MEDIATES METNASE
FUNCTION(S) IN NHEJ REPAIR

3.1. Wt-Metnase forms discrete nuclear foci at DSB sites

I next examined whether Metnase is localized at DNA damage sites following DSB damage. Human 293 cells over-expressing FLAG-Metnase were treated with IR (10 Gy), and the subcellular localization of FLAG-Metnase was determined at various times. In parallel, I stained for Nbs1, a member of the MRE11 complex that is known to be recruited to the DSB sites following IR (72, 112). Confocal microscopy showed that distinct nuclear foci of Metnase appeared within 2 hrs, peaking at 8 hrs post-irradiation (Figure 15B). Importantly, Metnase co-localized with Nbs1, a known DNA repair factor localized at DSB sites, following IR (112) (Figure 15A). I also observed a co-localization of Metnase with FancD2 (data not shown), another repair factor that was previously shown to co-localize with Nbs1 at DSB sites (72).

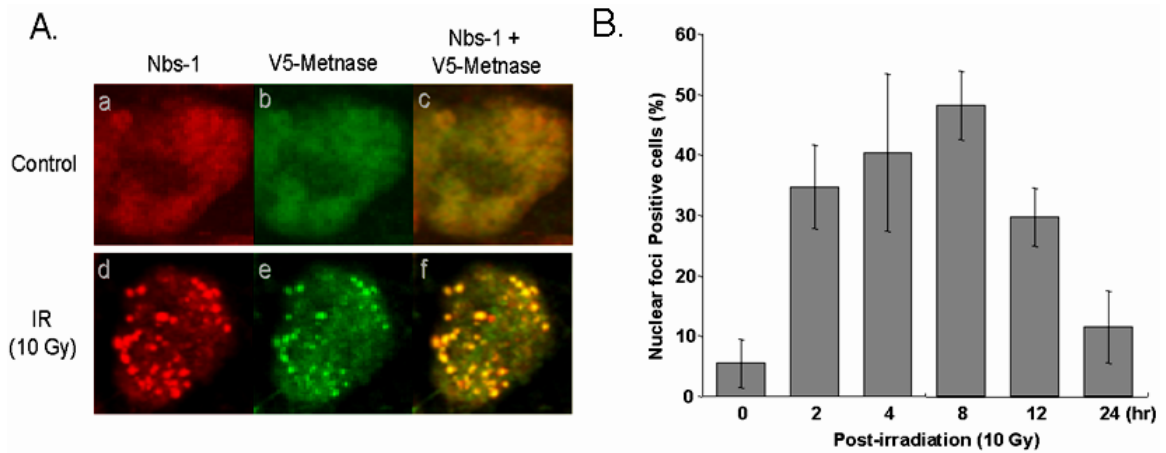


Figure 15. Nuclear localization of Metnase with Nbs1 following DSB. **A)** Human 293 cells over-expressing V5-Met were treated with 0 Gy (top) or 10 Gy (bottom) IR, and 8hrs later, cells were fixed and examined for Metnase and Nbs1. Images were obtained following double labeling of cells with polyclonal Ab to Nbs1 and monoclonal Ab to V5-epitope with Texas Red-conjugated anti-rabbit antibody (A and D) and fluorescein-conjugated anti-mouse antibody (B and E). The merged images were shown in C and F. **B)** IR-induced formation of discrete nuclear foci of Metnase. Human 293 cells over-expressing V5-Met were treated with of IR (10 Gy), and examined for nuclear localization of Metnase at various times.

3.2. hPso4 is a Metnase binding partner that redirects Metnase from TIR to non-TIR DNA

To identify Metnase binding partners, I carried out a co-immunoprecipitation experiment. Proteomic analysis identified 3 endogenous human proteins in the Metnase immunocomplexes (91): the 55-kDa human homolog of the PRP19 gene product of *S. cerevisiae* (PRP19/Pso4) involved in pre-mRNA splicing and DNA repair (22, 98, 113); the 50-kDa cleavage product of Metnase; and the 37-kDa human homolog of Spf27, a member of the Prp19 core complex also involved in pre-mRNA splicing (98, 113) (Figure 16). Previous papers had indicated that decreased levels of hPso4 expression negatively impacted cell survival following DNA damage (22). In addition, the six WD-40 repeats in the hPso4 sequence suggested a potential protein scaffolding role for hPso4 in DNA repair complex formation (22). For these reasons, hPso4 was first chosen to examine as a potential Metnase binding partner, rather than Spf27.

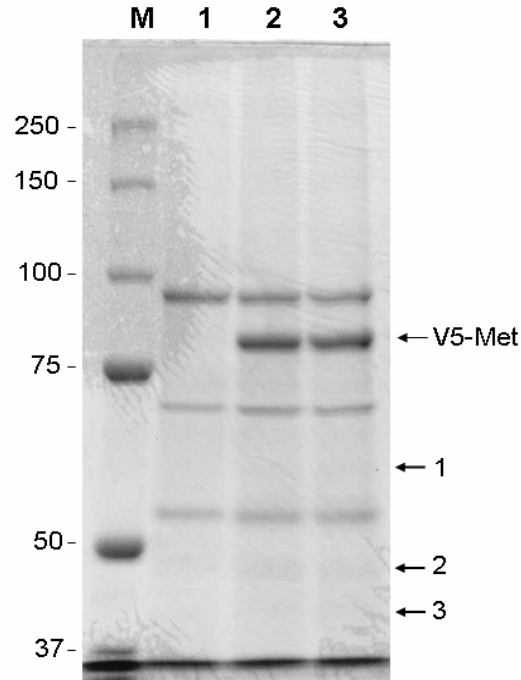


Figure 16. Immunoprecipitation of Metnase binding proteins. Whole cell extracts prepared from control 293 cells (lane 1) or cells stably expressing V5-Metnase (lanes 2 and 3) were incubated with 3 μ g of V5-monoclonal antibody at 4°C for 2 hrs, and further incubated overnight following addition of 100 μ L of Protein G-agarose beads. The complex was washed four times with 25 mM Tris-HCl (pH 7.5) containing 250 mM NaCl prior to running on a 10% SDS-PAGE and staining with Coomassie blue. Lane M represents molecular weight markers. Proteins 1, 2, and 3 were identified as Prp19, the gene product of *S. cerevisiae* (PRP19/Pso4), a cleavage product of Metnase (SETMAR), and the human homolog of Spf27, respectively. Experiment performed by Dr. Su-Jung Park.

To confirm the immunoprecipitation results, the hPso4 cDNA was cloned into a pFlag-CMV4 vector (Sigma). The hPso4-containing plasmid was first transfected into HEK293 cells using FuGENE6 transfection reagent, then selected for stable integration by propagation in media supplemented with G418 for three weeks. Individual growing colonies were selected and amplified to confluence in six-well dishes, and whole cell extracts were generated. Cell extracts were run on 10% SDS-PAGE, and Western blot analysis with Flag antibody confirmed the presence of the intact hPso4 protein (Figure 17A). A plasmid encoding V5-Metnase was then transfected into HEK293 cells stably expressing Flag-Pso4; Flag-Pso4 was transfected into cells stably expressing V5-Metnase. Cultures were allowed to incubate for 48 hours. Cells were lysed in 0.5% NP-40 lysis buffer and whole cell extracts were collected. 500 μ g of total protein was used to generate immunocomplexes with either anti-Flag or anti-V5 antibody. Protein G agarose beads were used to collect the immunocomplexes that were then run on 10% SDS-PAGE, transferred to nitrocellulose and probed with the indicated antibody (Figure 17B).

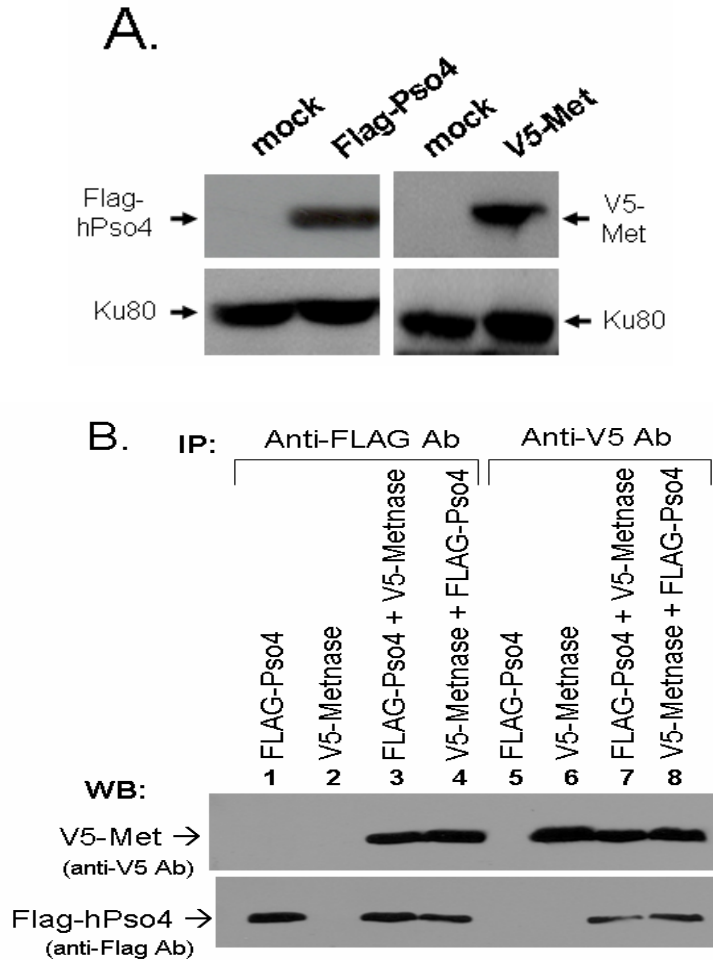


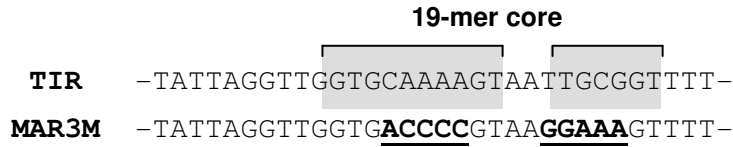
Figure 17. Physical association between Metnase and hPso4 on western blot. A) Western blot analysis of cells transfected with mock, Metnase- or hPso4-expressing vector. Ku80 was used as an internal loading control. **B)** Interaction of Metnase with hPso4. Whole cell extracts (100 μ g) from 293 cells over-expressing FLAG-Pso4 (lanes 1 and 5), V5-Metnase (lanes 2 and 6), or both (lanes 3, 4, 7, and 8) were incubated for 2 hrs with either anti-FLAG (lanes 1-4) or -V5 (lanes 5-8) antibody, then for an additional 2 hrs with Protein G-agarose. In lanes 3 and 7, human 293 cells over-expressing FLAG-Pso4 were transfected with a plasmid expressing V5-Metnase, whereas in lanes 4 and 8, cells over-expressing V5-Metnase were transfected with a plasmid expressing FLAG-Pso4. After elution, proteins were run on a 10% SDS-PAGE, transferred to membrane, and probed with either anti-V5 monoclonal (top panel) or -Pso4 polyclonal (bottom panel) antibody.

3.3. Metnase associates with non-TIR DNA in the presence of hPso4

Metnase can bind stably to dsDNA, but only at Terminal Inverted Repeat (TIR) sequences (Figure 18A). TIR sequences are unique to transposon proteins, and typically flank a movable genomic element on both sides. A transposase binds to the TIR sequence, excises the transposon sequence, then moves it elsewhere in the genome. This presumably was the original function of the Mariner-like domain of the Metnase fusion protein.

The specific TIR recognized by Metnase consists of a 19-mer core within a 32 base pair sequence (83) (Figure 18A). Mutations made to the 19-mer core of the TIR sequence decrease the stability of Metnase-DNA binding (Figure 18B and C). Specifically mutating two to three nucleotides at a time, I attempted to identify bases essential for Metnase association. Ultimately, nearly all of the mutations resulted in a significant reduction in Metnase binding affinity, but specific mutations at ten of the nineteen nucleotides were sufficient to completely abolish Metnase binding. The 32-mer dsDNA sequence containing these 10 mutations was called MAR3M.

A.



B.

DNA sequence of 19-mer of TIR core and mutants		Relative Metnase binding
TIR core	5'-GGTGCAAAGTAATTGCGG-3'	+++++
MARx4	- <u>CC</u> TGCAAAGTAATTGCGG-	++
MARx6	-GG <u>GT</u> CAAAAGTAATTGCGG-	+++
MARx7	-GGTG <u>AC</u> AAAAGTAATTGCGG-	+++
MARx8	-GGTGCAA <u>CC</u> GTAATTGCGG-	-
MARx9	-GGTGCAAAA <u>AG</u> AATTGCGG-	+++
MARx10	-GGTGCAAAGT <u>CC</u> TGCGG-	+++++
MARx11	-GGTGCAAAGTAAG <u>GG</u> GCGG-	++
MARx12	-GGTGCAAAGTAATT <u>AAA</u> G-	++
MAR1M	-GGTG <u>ACCCC</u> GTAATTGCGG-	-
MAR2M	-GGTGCAAAAAGTAA <u>GGAAA</u> G-	-
MAR3M	-GGTG <u>ACCCC</u> GTAAG <u>GGAAA</u> G-	-

C.

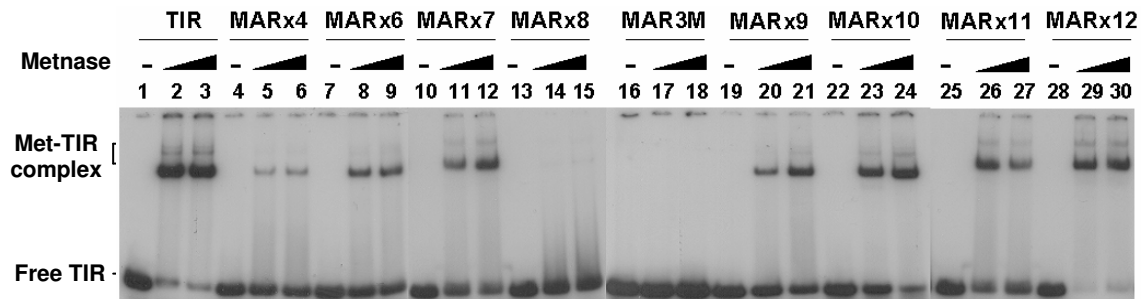


Figure 18. Metnase binds specifically to TIR dsDNA sequences. A) 5' TIR sequence of an Hsmar1 element. B) Mutations were designed to the TIR motif to identify the sequences necessary for stable Metnase binding. C) Electromobility shift assay examining binding of purified Metnase protein to 5'-radiolabeled TIR dsDNA and its mutants. Protein was incubated with labeled DNA in the presence of 50 mM Tris-Cl pH 7.5, 50 mM NaCl, 1 mM DTT, 0.2 mg/mL BSA, and 5% glycerol for 15 minutes, then analyzed on 5% native gel. Slower migrating bands indicate Metnase-TIR complex.

Previous reports have indicated that hPso4 possesses a sequence-independent binding to double-stranded DNA, but not single-stranded DNA (22). The results were not conclusive as the authors only tested plasmid DNA and 50-mer oligonucleotide DNA. To test the hPso4 protein myself, I purified Flag-Pso4 protein from HEK293 cells stably expressing the protein. Cells were lysed in a buffer containing 0.5% NP-40, subjected to dounce homogenization 25 times with B pestle, and soluble fractions clarified by high-speed centrifugation for one hour at 4°C. The supernate was incubated with anti-Flag antibody, loaded onto a protein G agarose column, washed with five column volumes of wash buffer, and bound protein was eluted competitively with Flag peptide (500 ng/μL). Eluted Flag-Pso4 was dialyzed against 10% glycerol, 0.01% NP-40, and 100 μM DTT and stored at -80°C. Radiolabeled single-stranded and double-stranded MAR3M DNA was then used to examine Pso4-DNA binding affinity, with results confirming those previously reported demonstrating sequence-independent binding to dsDNA, but not ssDNA (Figure 19A).

Given that hPso4 possesses a sequence-independent dsDNA binding activity and physically interacts with Metnase, I examined whether the Metnase-DNA interaction is influenced by hPso4. Addition of either protein alone to TIR dsDNA results in a slower migrating form of radiolabeled DNA corresponding to TIR bound to protein. When both Flag-hPso4 and V5-Metnase were incubated together prior to addition of labeled TIR DNA, a third band appeared, which migrated slower than either of the individual protein-DNA complexes (data not shown). Addition of either anti-Flag or anti-V5 antibody to the gel mobility shift assay reactions indicated the presence of both V5-Metnase and Flag-Pso4 in the slower migrating radiolabeled complexes. Furthermore, the presence of

supershifted bands following the addition of either V5- or Flag- antibody demonstrated that Metnase was able to form a stable complex with hPso4 on both TIR32 and non-TIR DNA (MAR3M) (Figure 19B). Previous research has indicated that hPso4 expression is induced upon DNA damage, lending support to the hypothesis that hPso4 could redirect the Metnase-DNA interaction from TIR to other non-TIR DNA including damaged DNA site(s).

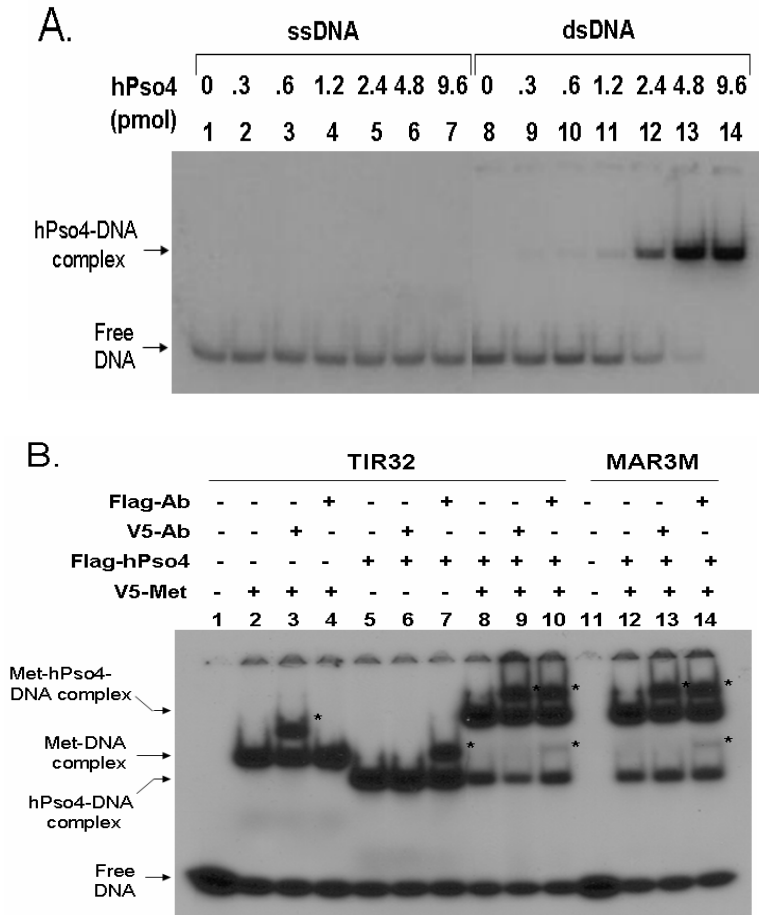


Figure 19. Stable complex formation on TIR and non-TIR DNA. **A)** Interaction of hPso4 with dsDNA and not ssDNA. Reaction mixtures (20 μ L) containing increasing amounts of hPso4 and 200 fmol of 5'- 32 P-labeled ssDNA (top strand of MAR3M) or dsDNA (MAR3M duplex DNA) were incubated for 15 min at 25°C and analyzed by 5% PAGE. **B)** Metnase forms a stable complex with hPso4 on both TIR and non-TIR DNA. Reaction mixtures (20 μ L) containing Metnase (0.2 μ g) and/or hPso4 (0.2 μ g) were incubated with 1 μ g of V5- or Flag-antibody for 30 min at 25°C prior to addition of 200 fmol of 5'- 32 P-labeled DNA. After 15 min of incubation at 25°C samples were analyzed by 5% native PAGE. The slowest migrating band observed in the presence of V5-Metnase, Flag-hPso4, and dsDNA (TIR32 or MAR3M) was supershifted in the presence of either V5- or Flag antibody (lanes 9, 10, 13, and 14), indicating that Metnase and hPso4 form a stable complex on dsDNA. The antibody- protein-DNA complexes (supershift) were indicated as *.

3.4. hPso4 is crucial for localization of Metnase at DSB sites and DNA end joining

Since Metnase is localized at damage foci following induction of double-strand breaks (Figure 15A and 20B), I next examined whether hPso4 is necessary for Metnase to reach these DSB sites. Human 293 cells stably expressing Flag-Metnase were transfected with a control- or hPso4-siRNA. Forty-eight hours later, cells were treated with IR and examined for formation of nuclear foci of Metnase and Nbs1 at DSB sites. Consistent with previous data (Figure 15A), cells transfected with a control-siRNA showed distinct Metnase foci co-localized with Nbs1 following IR (Figure 20C, second row). Cells transfected with hPso4-siRNA showed a somewhat diminished formation of both Nbs1 and Metnase foci. However, Metnase did not co-localize with Nbs1 following IR (Figure 20C, fourth row). Together, this result suggests that the presence of hPso4 is necessary in order for Metnase to form foci at sites of DNA damage. Although the possibility of decreased Metnase expression still potentially exists, low basal levels of hPso4 do not affect Metnase expression, so the possibility of an effect following DNA damage seems unlikely. I hypothesize that the diminished foci response is due to the inability of Metnase to associate with non-TIR DNA in the absence of hPso4.

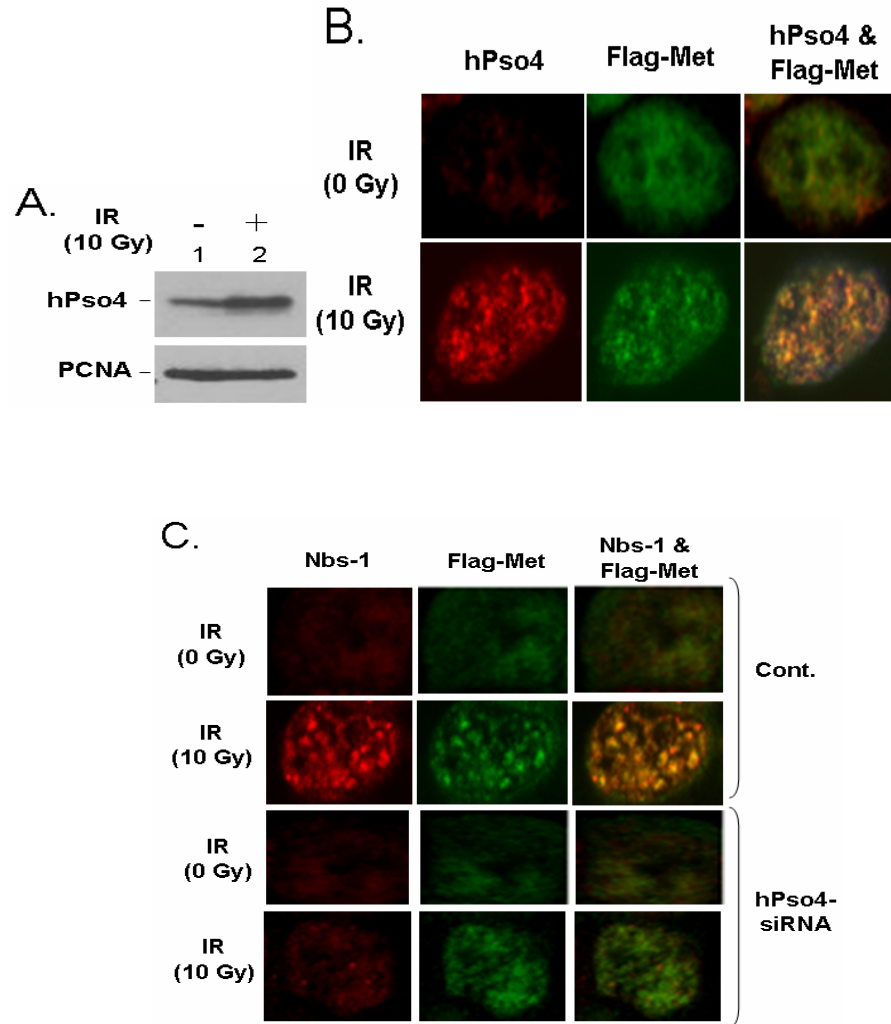


Figure 20. Metnase does not form foci *in vivo* in the absence of hPso4. **A)** Western analysis of IR-induced expression of hPso4. PCNA was used as a loading control. **B)** Co-localization of Metnase with hPso4 following DSB damage *in vivo*. Human 293 cells over-expressing Flag-Metnase were treated with 0 Gy (top panels) or 10 Gy (bottom panels) of IR. Following 8 hrs of incubation, cells were fixed and examined for cellular localization of Metnase and/or hPso4 using anti-Flag monoclonal (Sigma) and -hPso4 polyclonal (Merck, Darmstadt, Germany). Images were obtained following double labeling of fixed cells with polyclonal antibody to hPso4 and monoclonal antibody to Flag-epitope with Texas Red-conjugated anti-rabbit antibody and fluorescein-conjugated anti-mouse antibody. A co-localization of Metnase and hPso4 was examined using a Zeiss LSM-510 confocal microscopy. **C)** Effect of hPso4 on formation of discrete nuclear foci of Metnase at DSB sites. Human 293 cells stably expressing Flag-Metnase were treated with a control- or hPso4-siRNA for 48 hrs. Following 0 or 10 Gy of IR treatment, cells were examined for formation of nuclear foci of Metnase and Nbs1 at DSB sites.

To further understand the Metnase-hPso4 interaction with DNA, I examined the ability of a Metnase mutant lacking the SET domain (Met:dSET) for interaction with hPso4 on DNA. Met:dSET retained its TIR-binding activity, however it failed to form a complex with hPso4 on TIR or non-TIR DNA (Figure 21). These data suggest that the transposase domain essential for Metnase-TIR interaction is not sufficient for the Metnase-hPso4 interaction with either TIR or non-TIR DNA. The SET domain may be directly responsible for interaction with hPso4, although I was not able to test a mutant lacking transposase domain because it was unstable and quickly degraded (data not shown). Whether this degradation occurred *in vivo* or following cell lysis is unknown. If it were the latter, a larger quantity of cells could be grown and harvested in the cold room to potentially recover some measurable amount of protein.

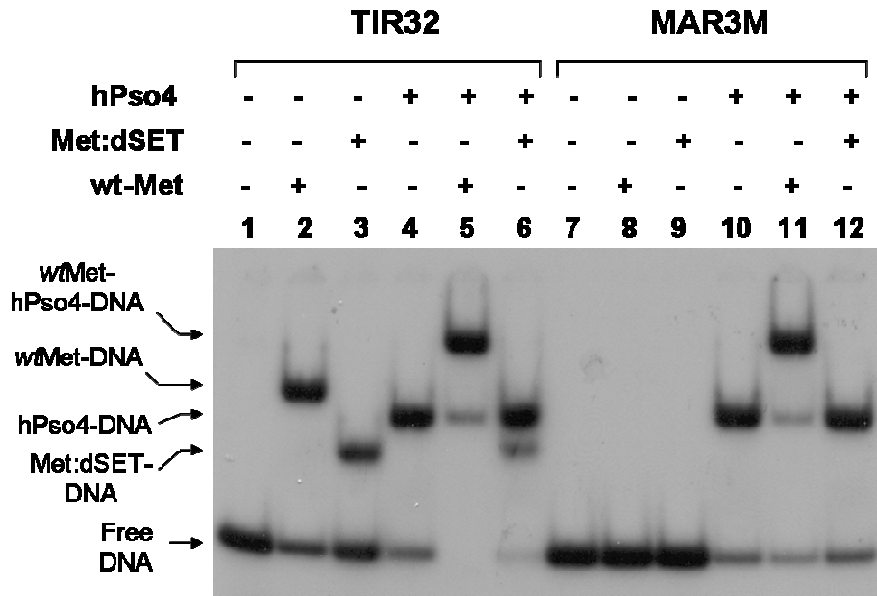


Figure 21. Transposase domain is not sufficient for Metnase-hPso4 binding.

Wt-Metnase or a mutant lacking the SET domain (Met:dSET) was incubated with ^{32}P -TIR (lanes 1-6) or non-TIR (^{32}P -MAR3M, lanes 7-12) in the absence or the presence of hPso4. Following a 15 min incubation, protein-DNA complexes were analyzed by 5% non-denaturing PAGE. Individual protein-DNA complexes were marked on the left side of the figure.

3.5. hPso4 is necessary for DNA end joining *in vivo* and *in vitro*

Pso4 is a dsDNA binding protein that plays a major but undefined role in mammalian DNA repair (22). My confocal microscopy study suggests that one of the roles of hPso4 in DSB repair is to introduce Metnase to DSB sites through a physical interaction (Figure 20B, C). This result prompted us to test whether hPso4 influences Metnase's function in DSB repair *in vivo*. Human 293 cells (1.0×10^5 per plate) were transfected with Metnase-siRNA, hPso4-siRNA, or a control-siRNA, and I examined how targeted inhibition of hPso4 expression would affect Metnase-mediated stimulation of *in vivo* end joining. Treatment of cells with hPso4-siRNA not only inhibited colony formation in mock cells, but also abolished Metnase-mediated stimulation of DNA end joining coupled to genomic integration (Figure 22B). Furthermore, extracts prepared from cells transfected with hPso4-siRNA, similar to those treated with Metnase-siRNA, failed to support DNA end joining *in vitro* (Figure 22C), suggesting that hPso4 has an indispensable role in DSB repair.

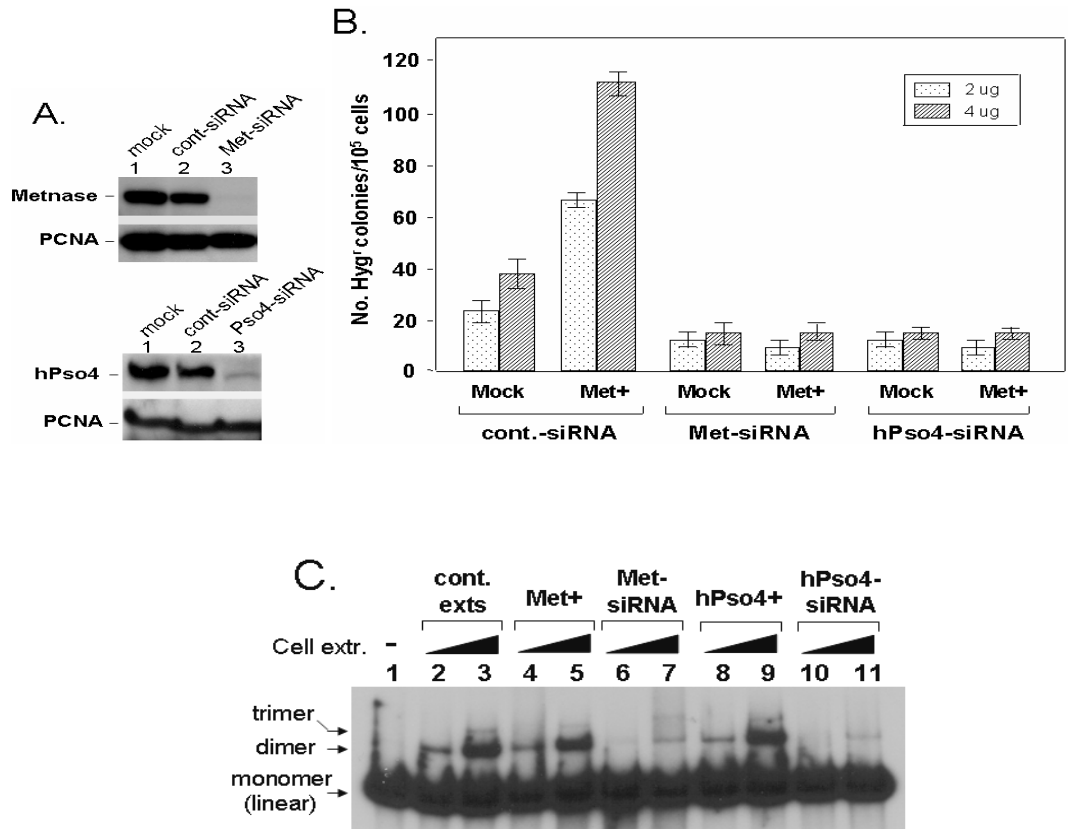


Figure 22. Lack of hPso4 negatively effects inter/intra-molecular end joining. **A)** HEK293 cells stably expressing either Flag-Metnase or Flag-hPso4 were transfected with siRNA for Metnase or hPso4, or scrambled control siRNA. Cell extracts were collected and analyzed by western blot using anti-Flag antibody. PCNA expression was used as a siRNA control. **B)** Mock HEK293 and Metnase over-expressor cells were treated with scrambled siRNA, Metnase siRNA, or hPso4 siRNA, and cell extracts were collected and used in a modified end-joining assay as described in Figure 2. **C)** Inter- and intra-molecular end joining with cell-free extracts. Different volumes of reaction mixtures contained 60 μ g of whole cell extracts (human 293 cells) and 20 ng of 5'-³²P-pBS DNA linearized with KpnI. Extracts consisted of either HEK293 (Cont. exts), Metnase-overexpressor (Met⁺), Metnase-underexpressor (Met-siRNA), hPso4-overexpressor (hPso4⁺), or hPso4-underexpressor (hPso4-siRNA). Reactions were incubated for 2 hr at 37°C, and DNA products were deproteinized and analyzed by 0.8% vertical agarose gel electrophoresis. Individual end joining products (circular- monomer, dimer, and trimer) were identified by T4 ligase-treated marker DNA.

Discussion:

Metnase is a SET and transposase fusion protein with histone lysine methyl transferase, sequence (TIR)-specific DNA binding, assembly of paired-end complex (PEC) and DNA cleavage activities (13). My *in vitro* and *in vivo* end joining studies have suggested that Metnase is involved in NHEJ. It remains uncertain how a protein that can only bind to DNA at specific sequences might function in genomic repair. In these experiments, I show that a second DNA repair factor, hPso4, is a binding partner for Metnase that allows it to associate with necessary non-TIR sequences. hPso4 is a human homolog of the *PS04/PRP19* gene in *S. cerevisiae* that has pleiotropic functions in DNA recombination and error-prone repair (22, 98, 113). hPso4 is induced by DNA damage, including IR and cisplatin (22), but also appears to exist at minimal levels intracellularly in the absence of DNA damage, for example as a nuclear matrix component (22, 95). Metnase and hPso4 function as DNA repair factors, both show enhanced chromatin association following DNA damage, and this along with our observation of a direct physical interaction (Figure 19B) suggest they might function together at sites of DSBs. Although hPso4 is a direct binding partner of Metnase, in our immunocomplexing assays of Metnase, the human homolog of Spf27, a member of the Prp19 core complex involved in pre-mRNA splicing (98, 113), was detected. hPso4 is also a member of the pre-mRNA splicing complex along with Cdc5L and Plrg1. It is currently unknown whether Metnase functions in this complex, or whether Spf27 was indirectly associated. The pre-mRNA splicing complex has been linked to V(D)J recombination through an association between hPso4 and terminal deoxytransferase (TdT) (22), which adds nucleotides to DNA ends (114-116). In addition, the pre-mRNA splicing complex has been linked to NHEJ through an association between

Cdc5L and WRN, a 3' → 5' exonuclease involved in DNA end processing (98). It is possible that the Metnase-hPso4 interaction is a part of a much larger complex that participates in DSB repair *in vivo*. One way to indirectly test this would be to clone another member of the pre-mRNA splicing complex into a tagged vector system and look for overlap in foci between it and Metnase following DNA damage. If this result were positive, knockdown assays of other members of the splicing complex would suggest whether the complex functioned alongside or in concert with Metnase.

Metnase recognizes the 19-mer core of the 5'-terminal inverted repeats (TIR) of the Hsmar1 element (Figure 18). Approximately half of the human genome derives from transposable elements, and there are over 7,000 potential Metnase binding sites in the human genome. The recruitment of the Metnase to the TIR sites may form a gene regulatory network that affects global gene expression in the absence of DNA damage (117). Once genomic damage is recognized, however, expression of hPso4 is upregulated (Figure 19A) and forms a stable complex with Metnase. Unlike Metnase, hPso4 has sequence-independent dsDNA binding activity, permitting Metnase to reach both TIR and non-TIR DNA equally (Figure 19B). Following IR treatment, Metnase formed discrete nuclear foci and co-localized with the MRN complex (Mre11-Rad50-Nbs1) (Figure 20C). Since one known function of the MRN complex is to recognize DNA damage and localize to those sites (72, 112), it is reasonable to conclude that the Metnase foci are occurring at sites of DSB damage. This could be confirmed using targeted DNA damage *in vivo*, then looking for Metnase accumulation at these sites under confocal microscope. Downregulation of hPso4 using siRNA prevented the localization of Metnase and Nbs1 to

damage sites (Figure 20C), suggesting that hPso4 interaction is essential for migration of Metnase to DSBs. Furthermore, the transposase domain of Metnase is not sufficient to allow the interaction with hPso4. A deletion mutant removing the SET domain from Metnase failed to interact with hPso4 on gel shift assay (Figure 21). It is currently unknown whether the SET domain alone is responsible for hPso4 interaction, or whether its presence is merely necessary for the two proteins to bind. The SET domain of Metnase is the domain responsible for TIR-specific DNA binding. Metnase cleavage activity comes from the transposase domain, so it remains to be seen whether the SET domain contributes to Metnase's function in DSB repair via histone lysine methyl transferase activity, interaction with hPso4, or both.

In these experiments, I showed that physical association of hPso4 with Metnase allows Metnase to localize to non-TIR regions in the genome, such as sites of DNA damage. Currently unanswered are questions regarding hPso4's influence on Metnase HLMT activity. Although hPso4 is upregulated following DNA damage, it exists at very low basal levels in the cell in the absence of damage, functioning as part of the nuclear matrix and in the pre-mRNA splicing complex. Our current work suggests that very little free hPso4 exists outside of these two components, but the physical interaction between the two proteins precludes dismissal of additional functional interactions between Metnase and hPso4. Pso4/Prp19 is a U-box protein with associated E3 ubiquitin ligase activity that is critical for its function in pre-mRNA splicing *in vivo* (113, 118-121). Given that ubiquitylation is rapidly induced at repair foci in response to DNA damage and can be detected using an antibody that specifically detects conjugated ubiquitin, hPso4's E3 ligase

activity may also play a role in DSB repair. It remains to be seen whether Metnase is a physiological substrate of hPso4.

AIM 4. *IN VITRO* ANALYSIS OF METNASE AND/OR HPSO4 BINDING TO DSDNA

4.1. Metnase exists as a dimer that mediates a synaptic complex with two TIRs in opposite orientation

The TIR-specific DNA binding activity of Metnase promotes a paired-end complex (PEC) of two TIR DNAs, suggesting that it functions as a dimer (18). To address the stoichiometric status of Metnase molecule(s), I examined whether Metnase molecules interact with each other *in vivo*. Using FuGENE6, a plasmid FLAG- or V5-Metnase was transfected using FuGENE6 into HEK293 cells stably expressing V5- or FLAG-Metnase, respectively. Cells were allowed to grow for 48 hours, then cells were lysed and extracts examined for interaction between Metnase molecules. FLAG- and V5-Metnase were co-immunoprecipitated by a reciprocal pull-down of Metnase using either anti-V5 or -FLAG antibody followed by probing with the reciprocal antibody upon western analysis (Figure 23). Results suggest that Metnase exists as more than one molecule *in vivo*.

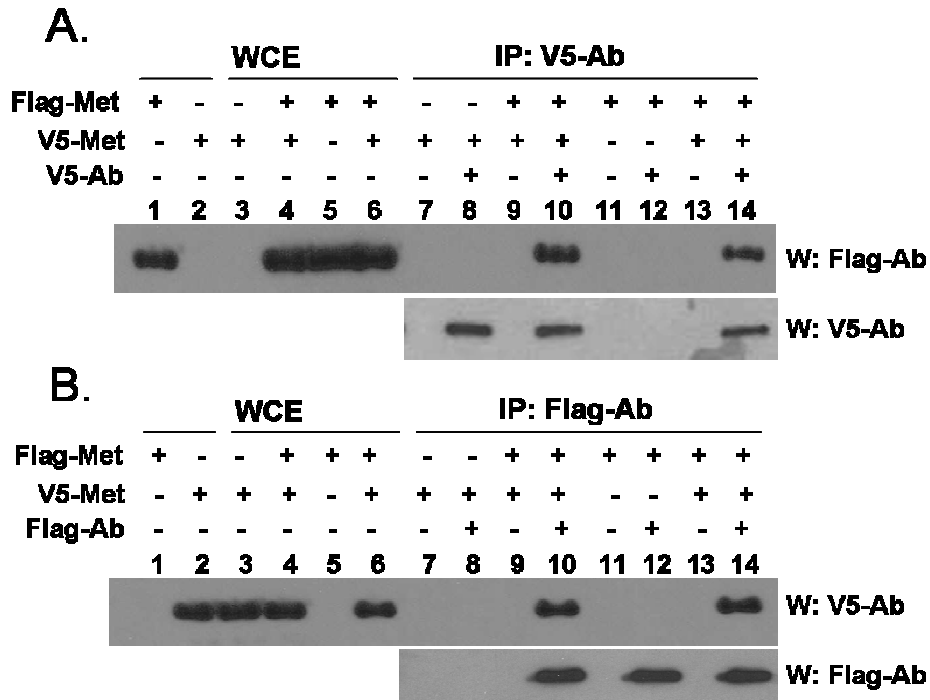


Figure 23. Physical interaction between Metnase molecules *in vivo*. Human 293 cells stably expressing V5-Metnase were transfected with a vector harboring Flag-Metnase, and 293 cells stably expressing Flag-Metnase were transfected with a vector expressing V5-Metnase. Forty-eight hours later, cell extracts were prepared and incubated with either an anti-V5 (panel A) or -Flag (panel B) monoclonal antibody for co-immunoprecipitation of V5- and Flag-Metnase. Following immunoprecipitation, samples were run on 10% SDS-PAGE and immunoblotted using either anti-Flag or -V5 antibody as indicated on the left side of the figure. In lanes 1-6, either purified Flag- or V5-Metnase (lanes 1 and 2) or whole cell extracts (WCE, lanes 3-6) were included as a loading control.

To determine whether Metnase actually exists as a dimer, I examined the native molecular mass of Metnase by glycerol gradient centrifugation. For this, purified Flag-Metnase was mixed with protein markers [urease (260 kDa, 11.8S), alcohol dehydrogenase (A.D., 150 kDa, 7.4S), bovine serum albumin (BSA, 67 kDa, 4.4S), and carbonic anhydrase (C.A., 29 kDa, 2.8S)] and sedimented on a 10-35% glycerol gradient by centrifugation at 45,500 rpm/4°C/26 hours. The migration of the 78 kDa Metnase was identified both by probing with anti-Flag on western blot, and by using its affinity for TIR DNA binding. After testing each of the gradient fractions, I determined that Metnase was eluted at the position of Alcohol dehydrogenase (150 kDa) (Figure 24). Taken together, the data indicate that Metnase indeed exists as a dimer.

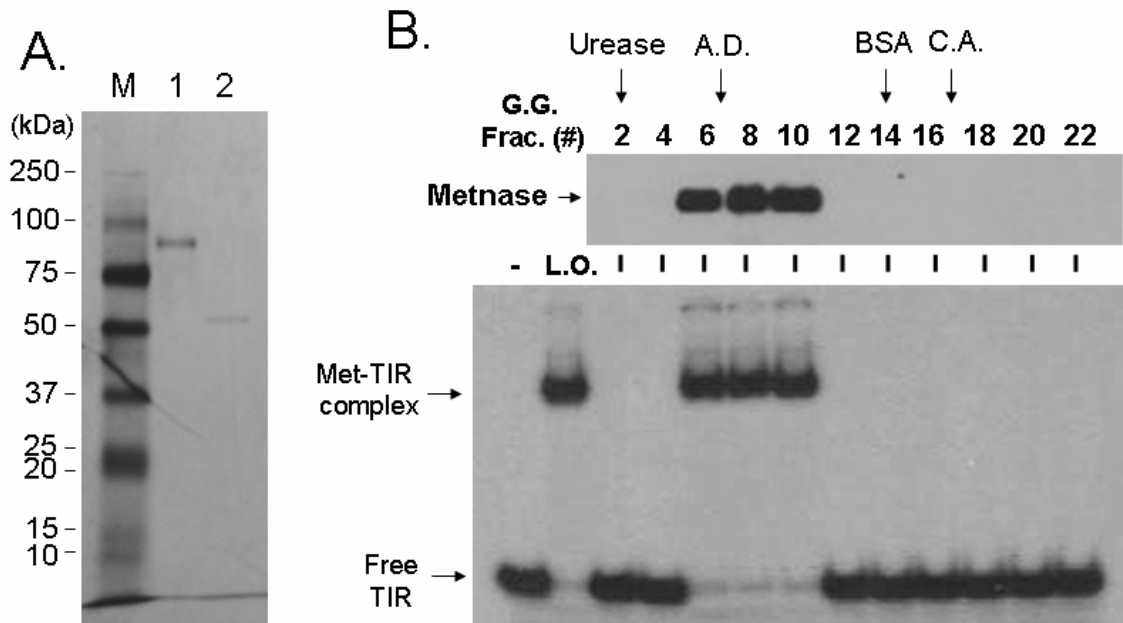


Figure 24. Glycerol gradient analysis of Metnase. Metnase and its TIR binding activity eluted at a dimer position on a glycerol gradient centrifugation. **A)** SDS-PAGE of immunopurified Flag-Metnase (lane 1) and Flag-hPso4 (lane 2) used in this study. Lane M represents protein markers. **B)** Glycerol gradient sedimentation of wt-Metnase. An aliquot of the immunopurified wt-Metnase was diluted with an equal volume of buffer B (50 mM Tris-HCl, pH 7.5, 5 mM DTT, 200 mM NaCl, 0.02% (w/v) NP40, and 0.5 mM EDTA, pH 8.0) containing protein markers [urease (260 kDa, 11.8S), alcohol dehydrogenase (A.D.; 150 kDa, 7.4S), bovine serum albumin (BSA; 67 kDa, 4.4S), and carbonic anhydrase (C.A.; 29 kDa, 2.8S)] and layered onto a 4.2-mL linear 10-35% (vol/vol) glycerol gradient. Gradients were centrifuged at 45,500 rpm for 26 hr in a Beckman SW55 rotor at 4°C. Fractions were collected from the bottom and analyzed for wt-Metnase (western blot, top panel) and TIR-specific DNA binding activity (bottom panel). Arrows marked indicate positions of protein markers. L.O. = load-on; protein before it was loaded onto the gradient.

The Metnase dimer supported a paired-end complex (PEC) with TIR DNA *in vitro*. Thus, I examined whether the Metnase dimer mediates formation of a synaptic complex with dsDNA containing two TIRs at the ends. For this, wt-Metnase was incubated with a double-stranded 118-mer oligonucleotide containing two 19-mer of TIR core at both ends, either with both TIRs running in a forward sequence (5' → 3') (FF-118), or with one TIR facing forward and the other running in reverse (3' → 5') (FR-118) (Figure 25A). Two distinct complexes were formed when Metnase was incubated with FF-118 containing two TIRs with same orientation. An incubation of Metnase with FR-118 containing two TIRs with opposite orientation produced only one complex (Figure 25B). Transposase sequence-specific DNA binding occurs in an orientation-dependent manner, Therefore, the result suggests that Metnase dimer induces DNA looping via a synaptic complex with DNA containing two TIRs in opposite orientation. Additional experiments could be performed to clarify this result. For instance, treatment with a restriction endonuclease in the region of sequence between the two TIR sequences might confirm the distinction between a looping structure and a 118-mer with only a single Metnase dimer attached. By labeling both the 5' and 3' ends of the 118-mer, if the looping model is correct, endonuclease restriction would result in a single radiolabeled species on an agarose gel. If, however, the model of a Metnase dimer sitting on only one TIR sequence is correct, then restriction would show two radiolabeled species – one quickly migrating, and one migrating much slower.

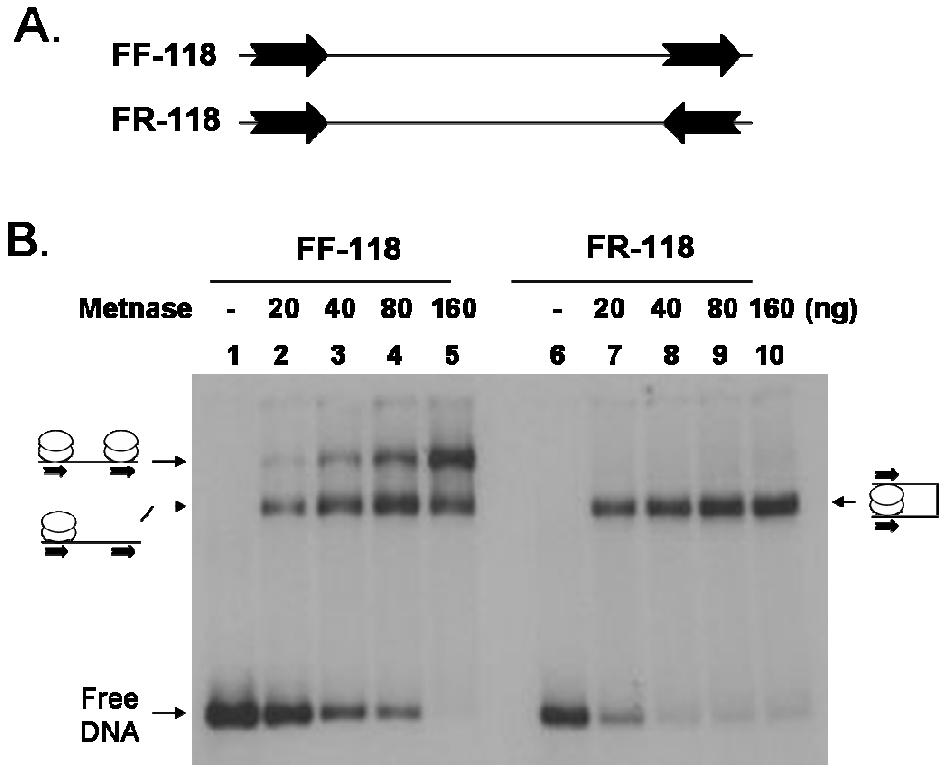


Figure 25. Metnase dimer interaction with dsDNA containing multiple TIRs. **A)** Two DNA substrates used in this study. FF-118 and FR-118 contain two 19-mer of TIR core with different orientations (indicated with arrows). **B)** Interaction of wt-Metnase with 200 fmol of either ^{32}P -labeled FF-118 (lanes 1-5) or ^{32}P -FR-118 (lanes 6-10) was examined using vertical 0.8% agarose gel electrophoresis. One or two molecules of Metnase dimer bound to the FF-118 were indicated on the left, while one Metnase dimer forming a synaptic complex with FR-118 was indicated on the right side.

4.2. Metnase forms a 1:1 stoichiometric complex with hPso4 on dsDNA

Metnase forms a stable interaction with hPso4 on DNA, and hPso4 is necessary for Metnase foci localization and repair function *in vivo*. Thus, I next investigated the physical characteristics of the Metnase-hPso4 interaction *in vitro*. Metnase showed TIR-specific DNA binding only (Figure 18C), while hPso4 interacted with dsDNA in a non-sequence-specific manner (Figure 19A). I further demonstrated the interaction between the Metnase-hPso4 complex with dsDNA. I carried out a stoichiometric analysis of Metnase and hPso4 binding to both TIR and non-TIR (MAR3M) DNA using gel mobility shift assays. Increasing amounts of hPso4 tetramer were added to a fixed amount of Flag-Metnase. The Metnase-hPso4-TIR complex formed in direct proportion to the increased amounts of hPso4-tetramer (*I21*) (0.25 to 2.0 pmol) in the presence of fixed amounts of Metnase (either 0.9 or 1.8 pmol) (Figure 26). Bands detected on the radioblots were excised and ³²P levels were measured by scintillation count to determine femtomoles of 32-mer present in each band. Plotting of protein-DNA complex versus hPso4 concentration showed a direct negative relationship between Metnase-TIR complex formation and hPso4 concentration. At the same time, Metnase-Pso4-TIR complex formation increased in an inverse manner. A similar result was obtained when non-TIR DNA (MAR3M) was used instead of TIR (Figure 27). Taken together, the data suggest that the Metnase dimer forms a 1:1 stoichiometric complex with hPso4-tetramer on dsDNA.

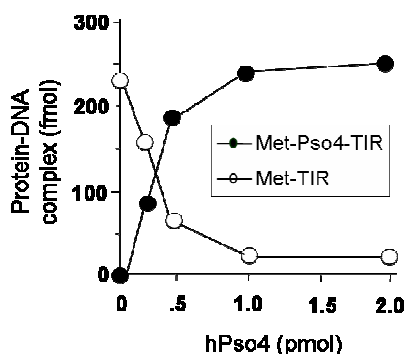
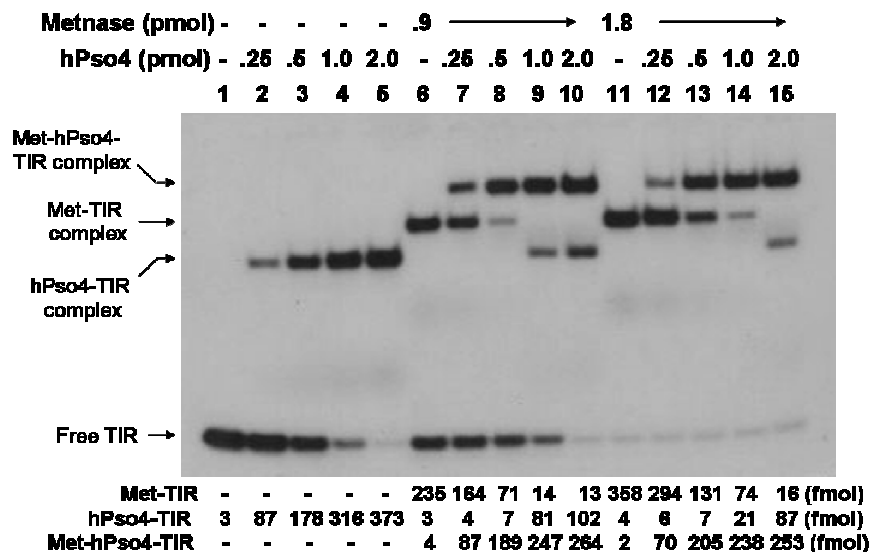


Figure 26. Metnase has 1:1 stoichiometry with hPso4 on TIR. Reaction mixtures (20 μ L) containing fixed amount of Metnase (0 or 0.9 pmol) were incubated with increasing amounts of hPso4 (0.25, 0.5, 1.0, and 2.0 pmol) for 15 min prior to addition of 400 fmol of 5'- 32 P-labeled DNA. Following 15 min incubation at 25°C, the protein-DNA complexes were analyzed by 5% native PAGE in the presence of 1X TBE. For quantification, individual bands were excised from dried gel and measured for radioactivity. In the lower panel, the amount of the Metnase-TIR and Metnase-hPso4-TIR complexes (fmol) were calculated.

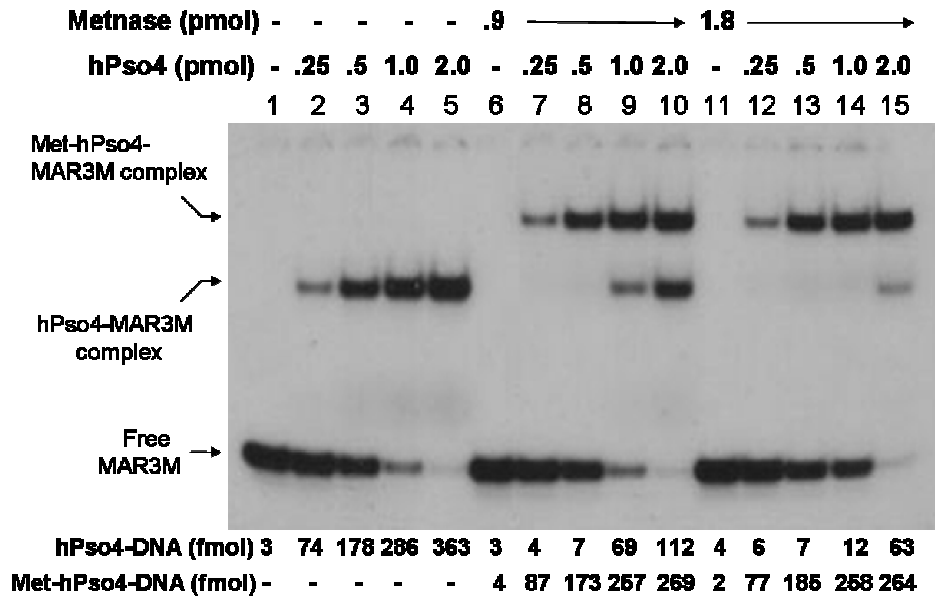


Figure 27. Titration of Metnase and hPso4 on non-TIR DNA. Reaction mixtures (20 μ L) were the same as those described in Figure 22, except for the use of 5' -³²P-labeled non-TIR DNA (MAR3M, 400 fmol) instead of TIR. Individual protein-DNA complexes were marked on the left side. For quantification, individual bands were excised from dried gel and measured for radioactivity.

4.3. hPso4, once forming a complex with Metnase, is solely responsible for binding to dsDNA

Metnase possesses TIR-specific DNA binding activity, whereas hPso4 binds to dsDNA with no sequence preference (22). Given that both Metnase and hPso4 bind to TIR DNA (Figure 19B), each protein in the Metnase-hPso4 complex may independently interact with TIR. Alternatively, only one protein in the Metnase-hPso4-TIR complex is responsible for DNA binding. To examine this, I carried out a stoichiometric analysis where Metnase, hPso4, and the Metnase-hPso4 complex were quantitatively analyzed for binding to TIR. Increasing stoichiometric amounts of both Metnase and hPso4 were added to 400 fmol ³²P-labeled TIR. The amount of TIR bound to each protein (Metnase or hPso4) was almost identical to those interacting with the Metnase-hPso4 two-protein complex (Figure 28). This experiment involves an excess of labeled DNA with protein as the limiting factor. If it were possible for both Metnase and hPso4 to associate with each other and still each bind DNA, the total femtomoles of ³²P-labeled TIR in the two-protein complex would have approached a two-fold increase over that measured in either single-protein DNA complex. However, the scintillation count of labeled DNA was nearly identical. This suggests that either Metnase or hPso4 sacrifices its ability to bind to DNA when it associates with its binding partner. The amount of TIR DNA bound to Metnase or hPso4 was also almost identical to those bound to the Metnase-hPso4 two-protein complex when increasing amounts of TIR were added to the reaction mixtures in the presence of fixed amounts of protein (Figure 29). Together, these results suggest that either Metnase or hPso4, but not both, is responsible for interacting with TIR DNA in formation of the Metnase-hPso4-TIR complex.

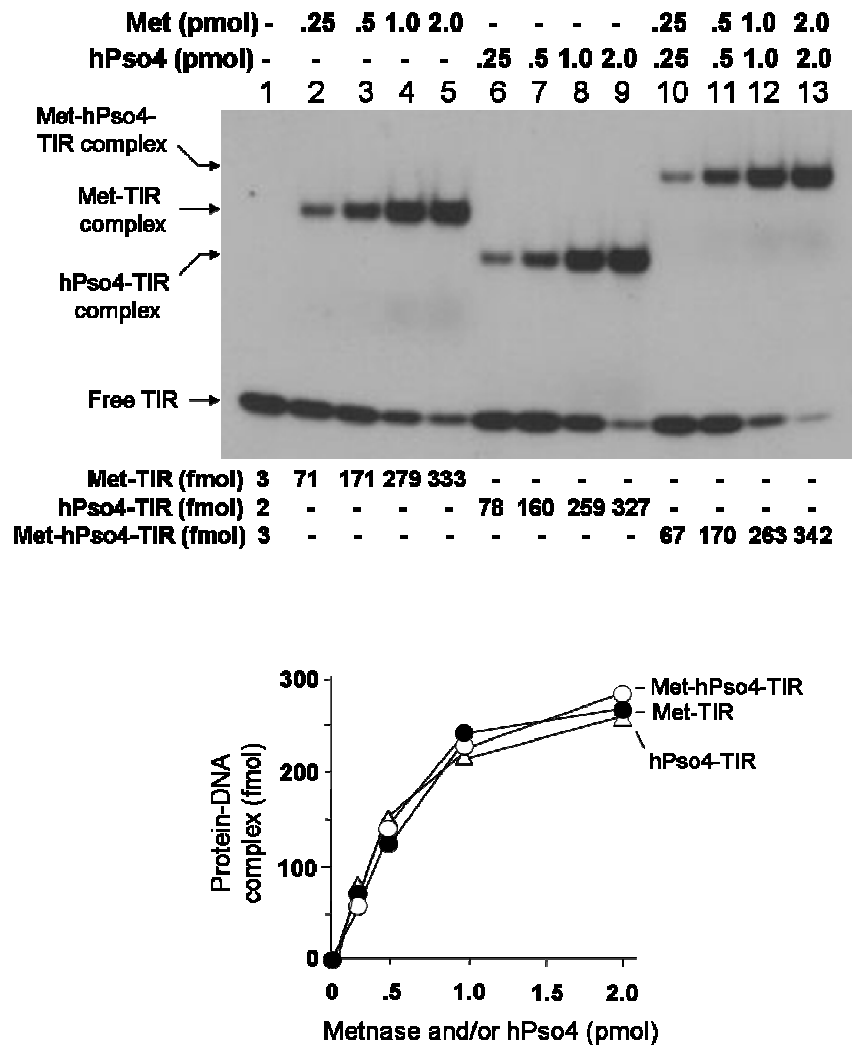


Figure 28. Stoichiometric analysis of Metnase and/or hPso4 bound to TIR DNA.

Stoichiometric analyses of binding of Metnase, hPso4, and the Metnase-hPso4 to TIR DNA. Reaction mixtures (20 μ L) containing indicated amounts of Metnase (lanes 2-5), hPso4 (lanes 6-9), or 1:1 mixture of Metnase-hPso4 (lanes 10-13) were incubated for 15 min at room temperature prior to addition of 400 fmol of 32 P-TIR DNA. After 15 min incubation, the protein-DNA complexes were analyzed by 5% native PAGE. Individual protein-DNA complexes (marked on the left side) were quantified following excision of individual bands from dried gel for measurement of radioactivity. In the lower panel, the Metnase-TIR, hPso4-TIR, and Metnase-hPso4-TIR complexes (fmol) were quantified.

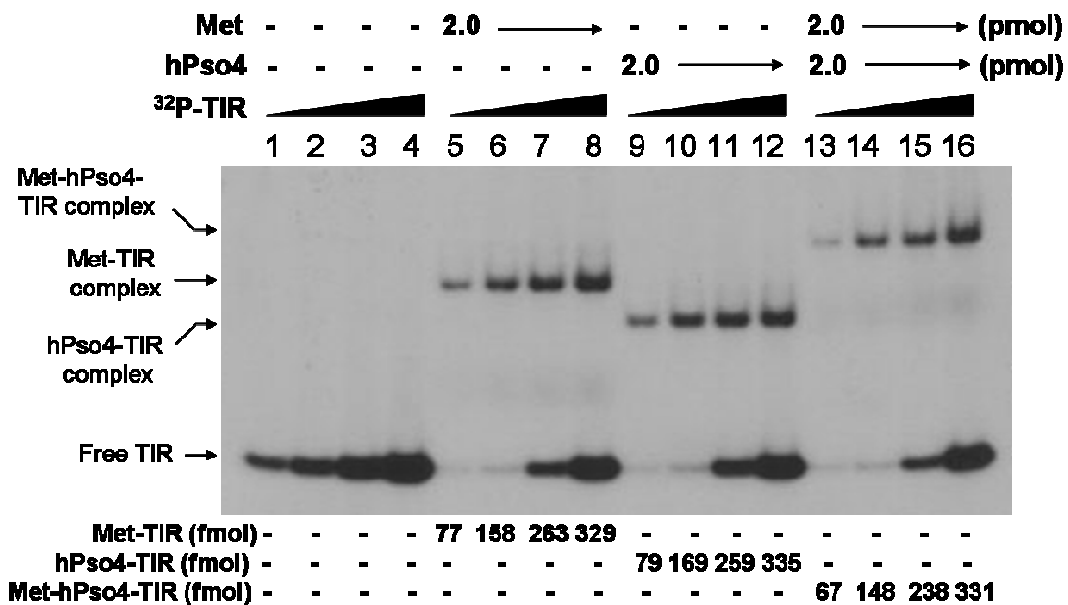


Figure 29. Relative binding activity of Metnase and hPso4, alone or together. Two pmol of Metnase, hPso4, or Metnase-hPso4 complex were pre-incubated at 25°C for 15 min before further incubation in the presence of increasing amounts (0.05, 0.1, 0.2, and 0.4 pmol) of ³²P-TIR DNA. Following incubation, the reaction mixtures were analyzed by 5% native PAGE. Individual protein-DNA complexes (marked on the left side of the figure) were quantified using the NIH image program (version 1.62).

I then examined which protein in the Metnase-hPso4-DNA complex is responsible for binding to DNA. For this, I compared the Metnase-hPso4 complex with hPso4 for quantitative binding to non-TIR DNA (MAR3M). The amount of MAR3M bound to hPso4 was almost identical to those bound to the Metnase-hPso4 complex (Figure 30A), suggesting that hPso4 in the Metnase-hPso4 complex is equally effective as free hPso4 in interaction with non-TIR DNA. Next, I carried out a competition experiment where the interaction of Metnase and/or hPso4 with ^{32}P -TIR DNA was examined in the presence of non-labeled competitor DNA. The Metnase- ^{32}P -TIR complex was significantly inhibited only in the presence of non-labeled TIR (Figure 30B, lanes 2-6), whereas formation of the hPso4- ^{32}P -TIR complex was competitively inhibited in the presence of both TIR and non-TIR DNA (Figure 30B, lanes 7-11). Similar to the hPso4-TIR, the Metnase-hPso4- ^{32}P -TIR two-protein complex was inhibited by both TIR and non-TIR DNA (Figure 30B, lanes 12-16), suggesting that hPso4 is solely responsible for binding to either TIR or non-TIR DNA in the Metnase-hPso4-DNA complex.

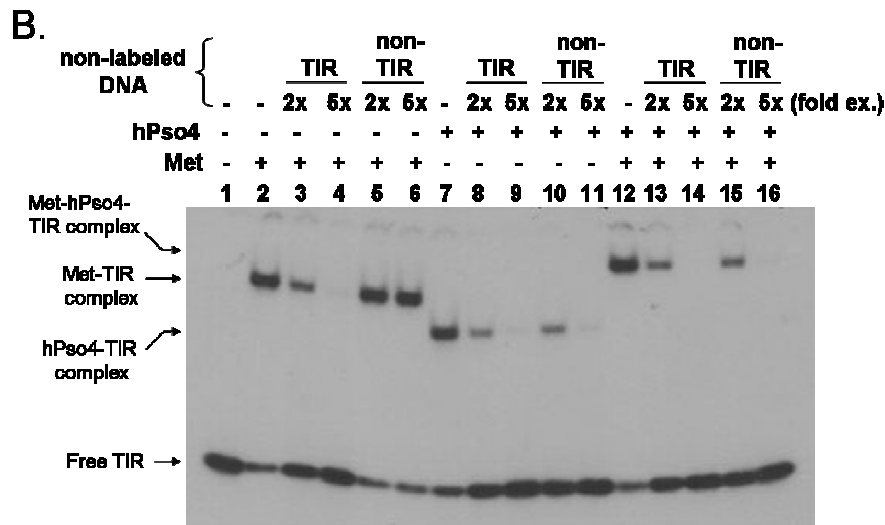
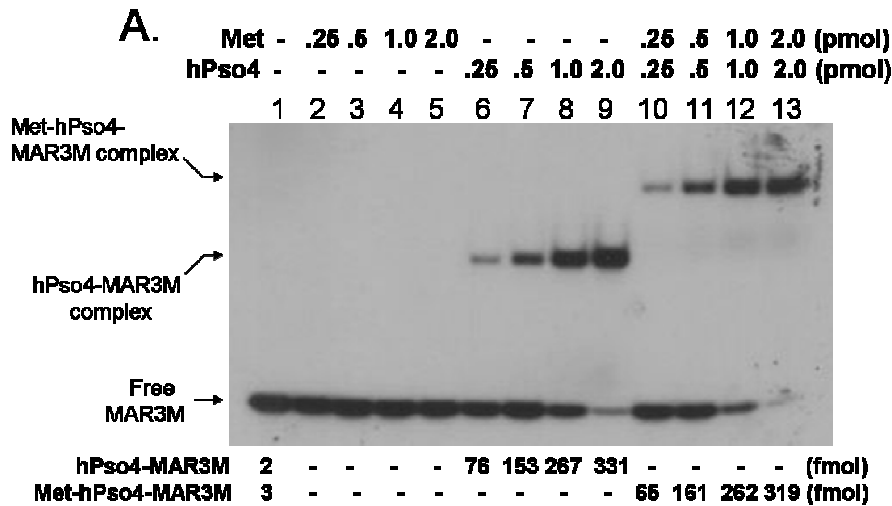


Figure 30. Protein interaction negatively influences Metnase-TIR binding. A)

Stoichiometric analysis of Metnase, hPso4, and the Metnase-hPso4 complex bound to non-TIR (MAR3M) DNA. Reaction mixtures (20 μ L) were the same as those indicated in Figure 24, except for the use of nonTIR DNA (MAR3M). Individual protein-DNA complexes (marked on the left side) were quantified following excision of individual bands from dried gel for measurement of radioactivity. **B)** The Metnase-hPso4-TIR complex is competitively inhibited by both TIR and non-TIR DNA. Metnase, hPso4, or the Metnase-hPso4 complex (2 pmol) was pre-incubated for 15 min at room temperature followed by an addition of 32 P-TIR DNA (200 fmol) in the presence of 2- or 5-fold excess of unlabeled TIR or non-TIR (MAR3M) DNA. Following 15 min incubation, the reaction mixtures were analyzed by 5% native PAGE. Individual protein-DNA complexes were marked on the left side.

4.4. hPso4 preferentially interacts with free Metnase over Metnase bound to TIR

The stoichiometric analyses shown in Figures 28-30 raised a question as to how hPso4 and not Metnase is responsible for dsDNA binding when the two proteins form a stable complex. One possibility is that hPso4, when in a complex with Metnase, prevents Metnase from binding to DNA. If so, Metnase already bound to DNA (TIR) may not be as effective as free Metnase in its ability to interact with hPso4. To test this possibility, I carried out an order of addition experiment. Metnase (or hPso4) was pre-incubated with DNA (TIR or non-TIR DNA) before or after addition of a stoichiometric amount of hPso4 (or Metnase), and was analyzed for formation of the Metnase-hPso4-DNA complex. When Metnase was pre-incubated with hPso4 or hPso4-DNA mixtures, most, if not all, of the Metnase protein was able to form a stable complex with hPso4 on dsDNA (TIR or non-TIR) (Figure 31, lanes 4, 6, 10, and 12). On the other hand, formation of the Metnase-hPso4-DNA complex was somewhat reduced when Metnase was pre-incubated with DNA before addition of hPso4 (Figure 31, lanes 5 and 11), suggesting that hPso4 preferentially interacts with free Metnase over Metnase bound to TIR.

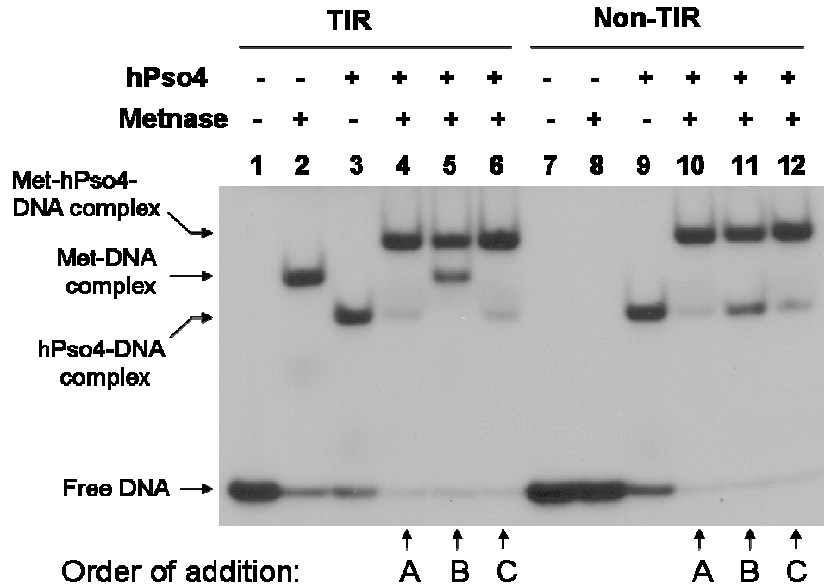


Figure 31. Metnase and hPso4 order of addition reaction. hPso4 preferentially interacts with free Metnase over Metnase bound to DNA. Two pmol of Metnase (lanes 2 and 8), hPso4 (lanes 3 and 9), or both (lanes 4-6 and 10-12) were incubated with 200 fmol of either TIR or nonTIR (MAR3M) DNA for formation of the protein(s)-DNA complexes. When both Metnase and hPso4 were present, the components were assembled in 3 separate ways: A (lanes 4 and 10), Metnase and hPso4 were preincubated for 15 min prior to addition of DNA; B (lanes 5 and 11), Metnase was preincubated with DNA first before addition of hPso4; C (lanes 6 and 12), hPso4 was incubation with DNA first, before addition of Metnase. Following 15 min incubation, the reaction mixtures were analyzed by 5% native PAGE. Individual protein-DNA complexes were marked on the left side.

To further understand this, I tested whether Metnase undergoes a conformational change upon binding to DNA. For this, wt-Metnase was examined for tryptic digestion patterns in the presence and absence of dsDNA. In the absence of DNA, wt-Metnase was cleaved into one major tryptic product (~40 kDa), however the 40 kDa cleavage product was further cleaved into smaller fragments (25 kDa and 15 kDa) in the presence of either TIR or non-TIR DNA (Figure 32). This result suggests that upon interaction with DNA, wild-type Metnase undergoes a conformational change that is not in favor of the Metnase-hPso4 interaction.

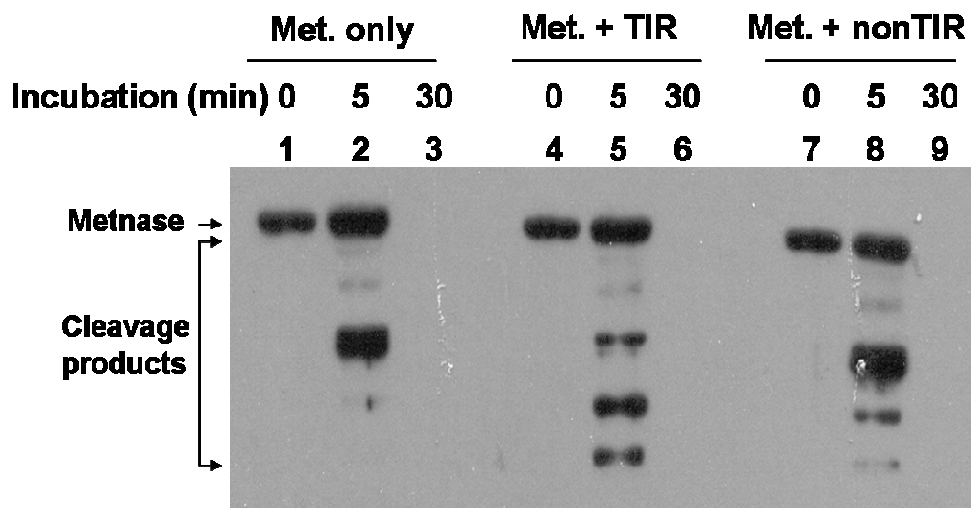


Figure 32. Trypsin digestion of Metnase in presence of TIR and non-TIR DNA.

Reaction mixtures (60 μ L) contained 0.1 M Tris-HCl (pH 8.5), and 100 ng/ μ L of wt-Flag-Metnase. Where indicated, 50 ng/ μ L of either TIR (lanes 4-6) or MAR3M (lanes 7-9) was added. After incubation at room temperature for 15 min, 50 ng of trypsin was added to the reaction. Reaction mixtures were then incubated at 37°C and aliquots were removed from the reactions at the indicated time points. Samples were mixed with gel loading buffer, boiled for 5 min, and loaded onto a 12% SDS-PAGE. The gel was then subjected to a Western blot analysis using an anti-FLAG monoclonal antibody.

Discussion:

This stoichiometric analysis has several interesting implications for the architecture of the Metnase-hPso4 complex on dsDNA. First, Metnase dimer forms a 1:1 stoichiometric complex with hPso4-tetramer on dsDNA (Figure 26). Although hPso4 is a direct binding partner of Metnase, Metnase also pulled down the human homolog of Spf27, a member of the Prp19 core complex involved in pre-mRNA splicing. Given that Pso4 is part of the pre-mRNA splicing complex consisting of Pso4, Cdc5L, Plrg1, and Spf27, the Metnase-hPso4 complex may be a part of the bigger complex including other members of the pre-mRNA splicing complex *in vivo*. Secondly, although both Metnase and hPso4 independently interact with TIR DNA, hPso4 is solely responsible for binding to dsDNA once the two proteins form a stable complex. This claim is based on the findings that i) the Metnase-hPso4 complex interacted with same stoichiometric amount of non-TIR DNA as the TIR DNA (Figure 26 and 27), ii) the Metnase-hPso4 complex interacted with same number of TIR molecules as Metnase or hPso4 alone did (Figure 28), and iii) formation of the Metnase-³²P-TIR complex was significantly inhibited by excess of TIR and not by non-TIR, whereas the Metnase-hPso4-TIR complexes were equally inhibited by both TIR and non-TIR DNA (Figure 30B).

It is not clear how Metnase's TIR binding activity is not functioning when it forms a complex with hPso4, although both Metnase and hPso4 possess very similar binding affinity to TIR DNA. It is possible that hPso4, once forming a complex with Metnase, may directly interfere with Metnase's DNA binding domain (helix-turn-helix motif). This notion is supported by a finding that Metnase bound to TIR DNA was less effective than

free Metnase in interacting with hPso4 (Figure 31). Further structural study would be necessary to clarify this intriguing issue. Considering that hPso4 is induced following IR treatment *in vivo* (22), formation of a stable Metnase-hPso4 complex likely occurs in response to DNA damage. Pso4 also undergoes structural alterations in response to DNA damage. The Metnase-hPso4 complex, once formed, likely goes to non-TIR sites such as sites of DNA double-strand breaks, since hPso4 is solely responsible for binding to DNA in forming the Metnase-hPso4-DNA complex. It would be interesting to see whether hPso4 also affects Metnase's other biochemical functions such as DNA cleavage activity and histone lysine methyl transferase activity.

Two separate roles for Metnase in NHEJ repair

Although the specific role Metnase plays in NHEJ repair is still not clear, a deletion of either the SET or the transposase domain abrogated its function in DNA repair, indicating that both domains are required for this function. Given that over-expression of Metnase promotes joining of both compatible- and non-compatible ends, I propose that Metnase has at least two separate functions in NHEJ repair (Figure 33). In the joining of compatible ends (I), Metnase-Lig4 interaction is induced following DNA damage, which promotes recruitment of the XRCC4-Lig4 complex, an essential player in the ligation step. Since wt-Metnase and not the D483A lacking DNA cleavage activity restores DNA end joining *in vivo* and *in vitro*, Metnase likely functions to promote the processing of non-compatible ends, a prerequisite step for the joining of non-compatible ends (II).

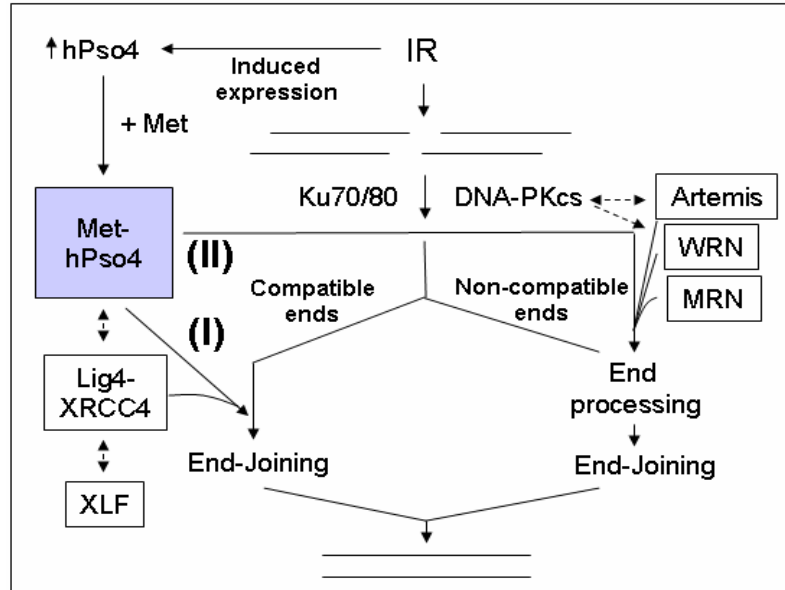


Figure 33. Proposed model of hPso4-Metnase function. Ionizing radiation causes double-strand breaks in cells, and also induces production of hPso4 by the cell. Increased levels of hPso4 favor binding to free Metnase, and the protein complex co-migrates to sites of damage. If the damaged ends are compatible (I), end-processing may not be necessary, and association with the DNA Ligase IV / XRCC4 complex and Cernunnos-XLF may be all that is required for re-ligation of the damaged strands. If the damaged ends are not compatible (II), processing of the ends is necessary before re-ligation can occur. Ku70/80 and the DNA-PK catalytic subunit are required, as well as Artemis, WRN protein, and the Mre11-Rad50-Nbs1 complex.

FUTURE DIRECTIONS:

While this work can serve as a basis for study of the functional and biochemical implications of the interaction between Metnase and hPso4, much work remains to be done. Currently the crystal structure analysis of Metnase is nearly complete, but the three-dimensional structure of the Pso4 tetramer remains a mystery. It would be interesting to determine the crystal structure of hPso4 to help identify the residues essential for interaction with Metnase. Similarly, this could lend insight into whatever conformational change is occurring in Metnase upon binding to TIR DNA, and why this change negatively influences the ability of hPso4 to bind.

The recent identification of phenylalanine 460 as the residue essential for Metnase dimerization has also suggested a number of new paths to follow. Purification of a mutant protein lacking the ability to dimerize will allow us to more closely examine the role of Metnase in global gene regulation by looking at up- and down-regulation of protein expression using a microarray system. The exact mechanism of DNA looping will also be settled. A Metnase mutant lacking the ability to dimerize will by necessity also lack the looping activity hypothesized in this work. In addition, a dimerization mutant will provide further insight into the role of Metnase in NHEJ. Addback of wild-type versus dimerization mutant Metnase to an *in vitro* end joining reaction will show whether Metnase must exist as a dimer in order to functionally assist in NHEJ. Specifically, does monomeric Metnase retain its cleavage activity? What implications does Metnase existing as a monomer versus a dimer have on cleavage of specific single-stranded DNA overhangs? It would also be

interesting to see how hPso4 is able to interact with Metnase, if at all. While monomeric Metnase may not be able to bind DNA by itself, perhaps Metnase could still reach sites of DNA damage through its interaction with Pso4.

Clearly Metnase and hPso4 both have roles in DNA repair that have not fully been realized. Hopefully these issues can be explored more thoroughly in the future.

REFERENCES:

1. D'Andrea, A. D., and Grompe, M. (2003) The Fanconi anaemia/BRCA pathway, *Nat Rev Cancer* 3, 23-34.
2. Gellert, M. (2002) V(D)J recombination: RAG proteins, repair factors, and regulation, *Annu Rev Biochem* 71, 101-132.
3. Lieber, M. R., Ma, Y., Pannicke, U., and Schwarz, K. (2003) Mechanism and regulation of human non-homologous DNA end-joining, *Nat Rev Mol Cell Biol* 4, 712-720.
4. Gottlich, B., Reichenberger, S., Feldmann, E., and Pfeiffer, P. (1998) Rejoining of DNA double-strand breaks in vitro by single-strand annealing, *Eur J Biochem* 258, 387-395.
5. Grawunder, U., Zimmer, D., Fugmann, S., Schwarz, K., and Lieber, M. R. (1998) DNA ligase IV is essential for V(D)J recombination and DNA double-strand break repair in human precursor lymphocytes, *Mol Cell* 2, 477-484.
6. Budman, J., and Chu, G. (2005) Processing of DNA for nonhomologous end-joining by cell-free extract, *Embo J* 24, 849-860.
7. Budman, J., Kim, S. A., and Chu, G. (2007) Processing of DNA for nonhomologous end-joining is controlled by kinase activity and XRCC4/ligase IV, *J Biol Chem* 282, 11950-11959.
8. Lee, S. H., and Kim, C. H. (2002) DNA-dependent protein kinase complex: a multifunctional protein in DNA repair and damage checkpoint, *Mol Cells* 13, 159-166.

9. Lees-Miller, S. P., and Meek, K. (2003) Repair of DNA double strand breaks by non-homologous end joining, *Biochimie* 85, 1161-1173.
10. Dai, Y., Kysela, B., Hanakahi, L. A., Manolis, K., Riballo, E., Stumm, M., Harville, T. O., West, S. C., Oettinger, M. A., and Jeggo, P. A. (2003) Nonhomologous end joining and V(D)J recombination require an additional factor, *Proc Natl Acad Sci U S A* 100, 2462-2467.
11. Liang, L., Deng, L., Nguyen, S. C., Zhao, X., Maulion, C. D., Shao, C., and Tischfield, J. A. (2008) Human DNA ligases I and III, but not ligase IV, are required for microhomology-mediated end joining of DNA double-strand breaks, *Nucleic Acids Res* 36, 3297-3310.
12. Tseng, S. F., Gabriel, A., and Teng, S. C. (2008) Proofreading activity of DNA polymerase Pol2 mediates 3'-end processing during nonhomologous end joining in yeast, *PLoS Genet* 4, e1000060.
13. Lee, S. H., Oshige, M., Durant, S. T., Rasila, K. K., Williamson, E. A., Ramsey, H., Kwan, L., Nickoloff, J. A., and Hromas, R. (2005) The SET domain protein Metnase mediates foreign DNA integration and links integration to nonhomologous end-joining repair, *Proc Natl Acad Sci U S A* 102, 18075-18080.
14. Williamson, E. A., Farrington, J., Martinez, L., Ness, S., O'Rourke, J., Lee, S. H., Nickoloff, J., and Hromas, R. (2008) Expression levels of the human DNA repair protein metnase influence lentiviral genomic integration, *Biochimie*.

15. Nakamura, T., Mori, T., Tada, S., Krajewski, W., Rozovskaia, T., Wassell, R., Dubois, G., Mazo, A., Croce, C. M., and Canaani, E. (2002) ALL-1 is a histone methyltransferase that assembles a supercomplex of proteins involved in transcriptional regulation, *Mol Cell* 10, 1119-1128.
16. Nishioka, K., Rice, J. C., Sarma, K., Erdjument-Bromage, H., Werner, J., Wang, Y., Chuikov, S., Valenzuela, P., Tempst, P., Steward, R., Lis, J. T., Allis, C. D., and Reinberg, D. (2002) PR-Set7 is a nucleosome-specific methyltransferase that modifies lysine 20 of histone H4 and is associated with silent chromatin, *Mol Cell* 9, 1201-1213.
17. Wang, H., Cao, R., Xia, L., Erdjument-Bromage, H., Borchers, C., Tempst, P., and Zhang, Y. (2001) Purification and functional characterization of a histone H3-lysine 4-specific methyltransferase, *Mol Cell* 8, 1207-1217.
18. Liu, D., Bischerour, J., Siddique, A., Buisine, N., Bigot, Y., and Chalmers, R. (2007) The human SETMAR protein preserves most of the activities of the ancestral Hsmar1 transposase, *Mol Cell Biol* 27, 1125-1132.
19. Miskey, C., Papp, B., Mates, L., Sinzelle, L., Keller, H., Izsvak, Z., and Ivics, Z. (2007) The ancient mariner sails again: transposition of the human Hsmar1 element by a reconstructed transposase and activities of the SETMAR protein on transposon ends, *Mol Cell Biol* 27, 4589-4600.
20. Roman, Y., Oshige, M., Lee, Y. J., Goodwin, K., Georgiadis, M. M., Hromas, R. A., and Lee, S. H. (2007) Biochemical characterization of a SET and transposase fusion protein, Metnase: its DNA binding and DNA cleavage activity, *Biochemistry* 46, 11369-11376.

21. Grey, M., Dusterhoft, A., Henriques, J. A., and Brendel, M. (1996) Allelism of PSO4 and PRP19 links pre-mRNA processing with recombination and error-prone DNA repair in *Saccharomyces cerevisiae*, *Nucleic Acids Res* 24, 4009-4014.
22. Mahajan, K. N., and Mitchell, B. S. (2003) Role of human Pso4 in mammalian DNA repair and association with terminal deoxynucleotidyl transferase, *Proc Natl Acad Sci U S A* 100, 10746-10751.
23. Daley, J. M., Palmbo, P. L., Wu, D., and Wilson, T. E. (2005) Nonhomologous end joining in yeast, *Annu Rev Genet* 39, 431-451.
24. Thompson, L. H., and Schild, D. (2001) Homologous recombinational repair of DNA ensures mammalian chromosome stability, *Mutat Res* 477, 131-153.
25. Takata, M., Sasaki, M. S., Sonoda, E., Morrison, C., Hashimoto, M., Utsumi, H., Yamaguchi-Iwai, Y., Shinohara, A., and Takeda, S. (1998) Homologous recombination and non-homologous end-joining pathways of DNA double-strand break repair have overlapping roles in the maintenance of chromosomal integrity in vertebrate cells, *Embo J* 17, 5497-5508.
26. Chlebowicz, E., and Jachymczyk, W. J. (1979) Repair of MMS-induced DNA double-strand breaks in haploid cells of *Saccharomyces cerevisiae*, which requires the presence of a duplicate genome, *Mol Gen Genet* 167, 279-286.
27. Hall, J. D., and Scherer, K. (1981) Repair of psoralen-treated DNA by genetic recombination in human cells infected with herpes simplex virus, *Cancer Res* 41, 5033-5038.

28. Livneh, Z., and Lehman, I. R. (1982) Recombinational bypass of pyrimidine dimers promoted by the recA protein of *Escherichia coli*, *Proc Natl Acad Sci U S A* 79, 3171-3175.
29. Resnick, M. A., and Moore, P. D. (1979) Molecular recombination and the repair of DNA double-strand breaks in CHO cells, *Nucleic Acids Res* 6, 3145-3160.
30. Feldmann, E., Schmiemann, V., Goedecke, W., Reichenberger, S., and Pfeiffer, P. (2000) DNA double-strand break repair in cell-free extracts from Ku80-deficient cells: implications for Ku serving as an alignment factor in non-homologous DNA end joining, *Nucleic Acids Res* 28, 2585-2596.
31. Moore, J. K., and Haber, J. E. (1996) Cell cycle and genetic requirements of two pathways of nonhomologous end-joining repair of double-strand breaks in *Saccharomyces cerevisiae*, *Mol Cell Biol* 16, 2164-2173.
32. Aoufouchi, S., Patrick, T., Lindsay, H. D., Shall, S., and Ford, C. C. (1997) Post-translational activation of non-homologous DNA end-joining in *Xenopus* oocyte extracts, *Eur J Biochem* 247, 518-525.
33. Lukacsovich, T., Yang, D., and Waldman, A. S. (1994) Repair of a specific double-strand break generated within a mammalian chromosome by yeast endonuclease I-SceI, *Nucleic Acids Res* 22, 5649-5657.
34. Smider, V., Rathmell, W. K., Lieber, M. R., and Chu, G. (1994) Restoration of X-ray resistance and V(D)J recombination in mutant cells by Ku cDNA, *Science* 266, 288-291.

35. Taccioli, G. E., Gottlieb, T. M., Blunt, T., Priestley, A., Demengeot, J., Mizuta, R., Lehmann, A. R., Alt, F. W., Jackson, S. P., and Jeggo, P. A. (1994) Ku80: product of the XRCC5 gene and its role in DNA repair and V(D)J recombination, *Science* 265, 1442-1445.
36. Featherstone, C., and Jackson, S. P. (1999) Ku, a DNA repair protein with multiple cellular functions?, *Mutat Res* 434, 3-15.
37. Labhart, P. (1999) Ku-dependent nonhomologous DNA end joining in *Xenopus* egg extracts, *Mol Cell Biol* 19, 2585-2593.
38. Wilson, T. E., Grawunder, U., and Lieber, M. R. (1997) Yeast DNA ligase IV mediates non-homologous DNA end joining, *Nature* 388, 495-498.
39. Daniel, R., Katz, R. A., Merkel, G., Hittle, J. C., Yen, T. J., and Skalka, A. M. (2001) Wortmannin potentiates integrase-mediated killing of lymphocytes and reduces the efficiency of stable transduction by retroviruses, *Mol Cell Biol* 21, 1164-1172.
40. DiBiase, S. J., Zeng, Z. C., Chen, R., Hyslop, T., Curran, W. J., Jr., and Iliakis, G. (2000) DNA-dependent protein kinase stimulates an independently active, nonhomologous, end-joining apparatus, *Cancer Res* 60, 1245-1253.
41. Hanakahi, L. A., Bartlet-Jones, M., Chappell, C., Pappin, D., and West, S. C. (2000) Binding of inositol phosphate to DNA-PK and stimulation of double-strand break repair, *Cell* 102, 721-729.
42. Hammarsten, O., and Chu, G. (1998) DNA-dependent protein kinase: DNA binding and activation in the absence of Ku, *Proc Natl Acad Sci U S A* 95, 525-530.

43. Hammarsten, O., DeFazio, L. G., and Chu, G. (2000) Activation of DNA-dependent protein kinase by single-stranded DNA ends, *J Biol Chem* 275, 1541-1550.
44. Hartley, K. O., Gell, D., Smith, G. C., Zhang, H., Divecha, N., Connelly, M. A., Admon, A., Lees-Miller, S. P., Anderson, C. W., and Jackson, S. P. (1995) DNA-dependent protein kinase catalytic subunit: a relative of phosphatidylinositol 3-kinase and the ataxia telangiectasia gene product, *Cell* 82, 849-856.
45. Goodarzi, A. A., Yu, Y., Riballo, E., Douglas, P., Walker, S. A., Ye, R., Harer, C., Marchetti, C., Morrice, N., Jeggo, P. A., and Lees-Miller, S. P. (2006) DNA-PK autophosphorylation facilitates Artemis endonuclease activity, *Embo J* 25, 3880-3889.
46. Ma, Y., Pannicke, U., Schwarz, K., and Lieber, M. R. (2002) Hairpin opening and overhang processing by an Artemis/DNA-dependent protein kinase complex in nonhomologous end joining and V(D)J recombination, *Cell* 108, 781-794.
47. Ma, Y., Schwarz, K., and Lieber, M. R. (2005) The Artemis:DNA-PKcs endonuclease cleaves DNA loops, flaps, and gaps, *DNA Repair (Amst)* 4, 845-851.
48. Paull, T. T., and Gellert, M. (1998) The 3' to 5' exonuclease activity of Mre 11 facilitates repair of DNA double-strand breaks, *Mol Cell* 1, 969-979.
49. Kamath-Loeb, A. S., Shen, J. C., Loeb, L. A., and Fry, M. (1998) Werner syndrome protein. II. Characterization of the integral 3' --> 5' DNA exonuclease, *J Biol Chem* 273, 34145-34150.

50. Shen, J. C., Gray, M. D., Oshima, J., Kamath-Loeb, A. S., Fry, M., and Loeb, L. A. (1998) Werner syndrome protein. I. DNA helicase and dna exonuclease reside on the same polypeptide, *J Biol Chem* 273, 34139-34144.
51. Yannone, S. M., Roy, S., Chan, D. W., Murphy, M. B., Huang, S., Campisi, J., and Chen, D. J. (2001) Werner syndrome protein is regulated and phosphorylated by DNA-dependent protein kinase, *J Biol Chem* 276, 38242-38248.
52. Cooper, M. P., Machwe, A., Orren, D. K., Brosh, R. M., Ramsden, D., and Bohr, V. A. (2000) Ku complex interacts with and stimulates the Werner protein, *Genes Dev* 14, 907-912.
53. Bebenek, K., Garcia-Diaz, M., Blanco, L., and Kunkel, T. A. (2003) The frameshift infidelity of human DNA polymerase lambda. Implications for function, *J Biol Chem* 278, 34685-34690.
54. Lee, J. W., Blanco, L., Zhou, T., Garcia-Diaz, M., Bebenek, K., Kunkel, T. A., Wang, Z., and Povirk, L. F. (2004) Implication of DNA polymerase lambda in alignment-based gap filling for nonhomologous DNA end joining in human nuclear extracts, *J Biol Chem* 279, 805-811.
55. Mahajan, K. N., Nick McElhinny, S. A., Mitchell, B. S., and Ramsden, D. A. (2002) Association of DNA polymerase mu (pol mu) with Ku and ligase IV: role for pol mu in end-joining double-strand break repair, *Mol Cell Biol* 22, 5194-5202.
56. Zhang, Y., Wu, X., Yuan, F., Xie, Z., and Wang, Z. (2001) Highly frequent frameshift DNA synthesis by human DNA polymerase mu, *Mol Cell Biol* 21, 7995-8006.

57. Grawunder, U., Wilm, M., Wu, X., Kulesza, P., Wilson, T. E., Mann, M., and Lieber, M. R. (1997) Activity of DNA ligase IV stimulated by complex formation with XRCC4 protein in mammalian cells, *Nature* 388, 492-495.
58. Grawunder, U., Zimmer, D., Kulesza, P., and Lieber, M. R. (1998) Requirement for an interaction of XRCC4 with DNA ligase IV for wild-type V(D)J recombination and DNA double-strand break repair in vivo, *J Biol Chem* 273, 24708-24714.
59. Wang, Y. G., Nnakwe, C., Lane, W. S., Modesti, M., and Frank, K. M. (2004) Phosphorylation and regulation of DNA ligase IV stability by DNA-dependent protein kinase, *J Biol Chem* 279, 37282-37290.
60. Junop, M. S., Modesti, M., Guarne, A., Ghirlando, R., Gellert, M., and Yang, W. (2000) Crystal structure of the Xrcc4 DNA repair protein and implications for end joining, *Embo J* 19, 5962-5970.
61. Teo, S. H., and Jackson, S. P. (1997) Identification of *Saccharomyces cerevisiae* DNA ligase IV: involvement in DNA double-strand break repair, *Embo J* 16, 4788-4795.
62. Ahnesorg, P., Smith, P., and Jackson, S. P. (2006) XLF interacts with the XRCC4-DNA ligase IV complex to promote DNA nonhomologous end-joining, *Cell* 124, 301-313.
63. Callebaut, I., Malivert, L., Fischer, A., Mornon, J. P., Revy, P., and de Villartay, J. P. (2006) Cernunnos interacts with the XRCC4 x DNA-ligase IV complex and is homologous to the yeast nonhomologous end-joining factor Nej1, *J Biol Chem* 281, 13857-13860.

64. Buck, D., Malivert, L., de Chasseval, R., Barraud, A., Fondaneche, M. C., Sanal, O., Plebani, A., Stephan, J. L., Hufnagel, M., le Deist, F., Fischer, A., Durandy, A., de Villartay, J. P., and Revy, P. (2006) Cernunnos, a novel nonhomologous end-joining factor, is mutated in human immunodeficiency with microcephaly, *Cell* 124, 287-299.
65. Sekiguchi, J. M., and Ferguson, D. O. (2006) DNA double-strand break repair: a relentless hunt uncovers new prey, *Cell* 124, 260-262.
66. Gatei, M., Zhou, B. B., Hobson, K., Scott, S., Young, D., and Khanna, K. K. (2001) Ataxia telangiectasia mutated (ATM) kinase and ATM and Rad3 related kinase mediate phosphorylation of Brca1 at distinct and overlapping sites. In vivo assessment using phospho-specific antibodies, *J Biol Chem* 276, 17276-17280.
67. Li, S., Ting, N. S., Zheng, L., Chen, P. L., Ziv, Y., Shiloh, Y., Lee, E. Y., and Lee, W. H. (2000) Functional link of BRCA1 and ataxia telangiectasia gene product in DNA damage response, *Nature* 406, 210-215.
68. Morrison, C., Sonoda, E., Takao, N., Shinohara, A., Yamamoto, K., and Takeda, S. (2000) The controlling role of ATM in homologous recombinational repair of DNA damage, *Embo J* 19, 463-471.
69. Fernandez-Capetillo, O., Mahadevaiah, S. K., Celeste, A., Romanienko, P. J., Camerini-Otero, R. D., Bonner, W. M., Manova, K., Burgoyne, P., and Nussenzweig, A. (2003) H2AX is required for chromatin remodeling and inactivation of sex chromosomes in male mouse meiosis, *Dev Cell* 4, 497-508.

70. Paull, T. T., Rogakou, E. P., Yamazaki, V., Kirchgessner, C. U., Gellert, M., and Bonner, W. M. (2000) A critical role for histone H2AX in recruitment of repair factors to nuclear foci after DNA damage, *Curr Biol* 10, 886-895.
71. Buscemi, G., Savio, C., Zannini, L., Micciche, F., Masnada, D., Nakanishi, M., Tauchi, H., Komatsu, K., Mizutani, S., Khanna, K., Chen, P., Concannon, P., Chessa, L., and Delia, D. (2001) Chk2 activation dependence on Nbs1 after DNA damage, *Mol Cell Biol* 21, 5214-5222.
72. Mirzoeva, O. K., and Petrini, J. H. (2001) DNA damage-dependent nuclear dynamics of the Mre11 complex, *Mol Cell Biol* 21, 281-288.
73. Zhao, S., Weng, Y. C., Yuan, S. S., Lin, Y. T., Hsu, H. C., Lin, S. C., Gerbino, E., Song, M. H., Zdzienicka, M. Z., Gatti, R. A., Shay, J. W., Ziv, Y., Shiloh, Y., and Lee, E. Y. (2000) Functional link between ataxia-telangiectasia and Nijmegen breakage syndrome gene products, *Nature* 405, 473-477.
74. Bernstein, C., Bernstein, H., Payne, C. M., and Garewal, H. (2002) DNA repair/pro-apoptotic dual-role proteins in five major DNA repair pathways: fail-safe protection against carcinogenesis, *Mutat Res* 511, 145-178.
75. Katagiri, T., Saito, H., Shinohara, A., Ogawa, H., Kamada, N., Nakamura, Y., and Miki, Y. (1998) Multiple possible sites of BRCA2 interacting with DNA repair protein RAD51, *Genes Chromosomes Cancer* 21, 217-222.
76. Wong, A. K., Pero, R., Ormonde, P. A., Tavtigian, S. V., and Bartel, P. L. (1997) RAD51 interacts with the evolutionarily conserved BRC motifs in the human breast cancer susceptibility gene *brca2*, *J Biol Chem* 272, 31941-31944.

77. Yang, H., Jeffrey, P. D., Miller, J., Kinnucan, E., Sun, Y., Thoma, N. H., Zheng, N., Chen, P. L., Lee, W. H., and Pavletich, N. P. (2002) BRCA2 function in DNA binding and recombination from a BRCA2-DSS1-ssDNA structure, *Science* 297, 1837-1848.
78. Yang, H., Li, Q., Fan, J., Holloman, W. K., and Pavletich, N. P. (2005) The BRCA2 homologue Brh2 nucleates RAD51 filament formation at a dsDNA-ssDNA junction, *Nature* 433, 653-657.
79. Constantinou, A., Tarsounas, M., Karow, J. K., Brosh, R. M., Bohr, V. A., Hickson, I. D., and West, S. C. (2000) Werner's syndrome protein (WRN) migrates Holliday junctions and co-localizes with RPA upon replication arrest, *EMBO Rep* 1, 80-84.
80. Yang, Q., Zhang, R., Wang, X. W., Spillare, E. A., Linke, S. P., Subramanian, D., Griffith, J. D., Li, J. L., Hickson, I. D., Shen, J. C., Loeb, L. A., Mazur, S. J., Appella, E., Brosh, R. M., Jr., Karmakar, P., Bohr, V. A., and Harris, C. C. (2002) The processing of Holliday junctions by BLM and WRN helicases is regulated by p53, *J Biol Chem* 277, 31980-31987.
81. Lopes, M., Foiani, M., and Sogo, J. M. (2006) Multiple mechanisms control chromosome integrity after replication fork uncoupling and restart at irreparable UV lesions, *Mol Cell* 21, 15-27.
82. Muller, B., Boehmer, P. E., Emmerson, P. T., and West, S. C. (1991) Action of RecBCD enzyme on Holliday structures made by RecA, *J Biol Chem* 266, 19028-19033.

83. Cordaux, R., Udit, S., Batzer, M. A., and Feschotte, C. (2006) Birth of a chimeric primate gene by capture of the transposase gene from a mobile element, *Proc Natl Acad Sci U S A* *103*, 8101-8106.
84. Robertson, H. M., and Zumpano, K. L. (1997) Molecular evolution of an ancient mariner transposon, Hsmar1, in the human genome, *Gene* *205*, 203-217.
85. Nishioka, K., Chuikov, S., Sarma, K., Erdjument-Bromage, H., Allis, C. D., Tempst, P., and Reinberg, D. (2002) Set9, a novel histone H3 methyltransferase that facilitates transcription by precluding histone tail modifications required for heterochromatin formation, *Genes Dev* *16*, 479-489.
86. Min, J., Zhang, X., Cheng, X., Grewal, S. I., and Xu, R. M. (2002) Structure of the SET domain histone lysine methyltransferase Clr4, *Nat Struct Biol* *9*, 828-832.
87. Zhang, X., Tamaru, H., Khan, S. I., Horton, J. R., Keefe, L. J., Selker, E. U., and Cheng, X. (2002) Structure of the Neurospora SET domain protein DIM-5, a histone H3 lysine methyltransferase, *Cell* *111*, 117-127.
88. Jordan, I. K. (2006) Evolutionary tinkering with transposable elements, *Proc Natl Acad Sci U S A* *103*, 7941-7942.
89. Haren, L., Ton-Hoang, B., and Chandler, M. (1999) Integrating DNA: transposases and retroviral integrases, *Annu Rev Microbiol* *53*, 245-281.
90. Zhang, X., Yang, Z., Khan, S. I., Horton, J. R., Tamaru, H., Selker, E. U., and Cheng, X. (2003) Structural basis for the product specificity of histone lysine methyltransferases, *Mol Cell* *12*, 177-185.

91. Beck, B. D., Park, S. J., Lee, Y. J., Roman, Y., Hromas, R. A., and Lee, S. H. (2008) Human Pso4 is a metnase (SETMAR)-binding partner that regulates metnase function in DNA repair, *J Biol Chem* 283, 9023-9030.
92. Daniel, R., Greger, J. G., Katz, R. A., Taganov, K. D., Wu, X., Kappes, J. C., and Skalka, A. M. (2004) Evidence that stable retroviral transduction and cell survival following DNA integration depend on components of the nonhomologous end joining repair pathway, *J Virol* 78, 8573-8581.
93. Daniel, R., Katz, R. A., and Skalka, A. M. (1999) A role for DNA-PK in retroviral DNA integration, *Science* 284, 644-647.
94. Skalka, A. M., and Katz, R. A. (2005) Retroviral DNA integration and the DNA damage response, *Cell Death Differ* 12 Suppl 1, 971-978.
95. Gotzmann, J., Gerner, C., Meissner, M., Holzmann, K., Grimm, R., Mikulits, W., and Sauermann, G. (2000) hNMP 200: a novel human common nuclear matrix protein combining structural and regulatory functions, *Exp Cell Res* 261, 166-179.
96. Gerner, C., and Sauermann, G. (1999) Nuclear matrix proteins specific for subtypes of human hematopoietic cells, *J Cell Biochem* 72, 470-482.
97. Ajuh, P., Kuster, B., Panov, K., Zomerdijk, J. C., Mann, M., and Lamond, A. I. (2000) Functional analysis of the human CDC5L complex and identification of its components by mass spectrometry, *Embo J* 19, 6569-6581.
98. Zhang, N., Kaur, R., Lu, X., Shen, X., Li, L., and Legerski, R. J. (2005) The Pso4 mRNA splicing and DNA repair complex interacts with WRN for processing of DNA interstrand cross-links, *J Biol Chem* 280, 40559-40567.

99. Park, S. J., Ciccone, S. L., Freie, B., Kurimasa, A., Chen, D. J., Li, G. C., Clapp, D. W., and Lee, S. H. (2004) A positive role for the Ku complex in DNA replication following strand break damage in mammals, *J Biol Chem* 279, 6046-6055.
100. Murti, K. G., He, D. C., Brinkley, B. R., Scott, R., and Lee, S. H. (1996) Dynamics of human replication protein A subunit distribution and partitioning in the cell cycle, *Exp Cell Res* 223, 279-289.
101. Guo, Y., Costa, R., Ramsey, H., Starnes, T., Vance, G., Robertson, K., Kelley, M., Reinbold, R., Scholer, H., and Hromas, R. (2002) The embryonic stem cell transcription factors Oct-4 and FoxD3 interact to regulate endodermal-specific promoter expression, *Proc Natl Acad Sci U S A* 99, 3663-3667.
102. Baumann, P., and West, S. C. (1998) DNA end-joining catalyzed by human cell-free extracts, *Proc Natl Acad Sci U S A* 95, 14066-14070.
103. Budman, J., and Chu, G. (2005) Processing of DNA for nonhomologous end-joining by cell-free extract, in *Embo J*, pp 849-860.
104. Budman, J., and Chu, G. (2006) Assays for nonhomologous end joining in extracts, *Methods Enzymol* 408, 430-444.
105. Paull, T. T., and Gellert, M. (1999) Nbs1 potentiates ATP-driven DNA unwinding and endonuclease cleavage by the Mre11/Rad50 complex, *Genes Dev* 13, 1276-1288.
106. Leiden, J. M., and Strominger, J. L. (1986) Generation of diversity of the beta chain of the human T-lymphocyte receptor for antigen, *Proc Natl Acad Sci U S A* 83, 4456-4460.

107. Malissen, M., McCoy, C., Blanc, D., Trucy, J., Devaux, C., Schmitt-Verhulst, A. M., Fitch, F., Hood, L., and Malissen, B. (1986) Direct evidence for chromosomal inversion during T-cell receptor beta-gene rearrangements, *Nature* 319, 28-33.
108. Yoshikai, Y., Clark, S. P., Taylor, S., Sohn, U., Wilson, B. I., Minden, M. D., and Mak, T. W. (1985) Organization and sequences of the variable, joining and constant region genes of the human T-cell receptor alpha-chain, *Nature* 316, 837-840.
109. Kobayashi, J., Antocchia, A., Tauchi, H., Matsuura, S., and Komatsu, K. (2004) NBS1 and its functional role in the DNA damage response, *DNA Repair (Amst)* 3, 855-861.
110. Li, L., Salido, E., Zhou, Y., Bhattacharyya, S., Yannone, S. M., Dunn, E., Meneses, J., Feeney, A. J., and Cowan, M. J. (2005) Targeted disruption of the Artemis murine counterpart results in SCID and defective V(D)J recombination that is partially corrected with bone marrow transplantation, *J Immunol* 174, 2420-2428.
111. Pannicke, U., Ma, Y., Hopfner, K. P., Niewolik, D., Lieber, M. R., and Schwarz, K. (2004) Functional and biochemical dissection of the structure-specific nuclease ARTEMIS, *Embo J* 23, 1987-1997.
112. Maser, R. S., Mirzoeva, O. K., Wells, J., Olivares, H., Williams, B. R., Zinkel, R. A., Farnham, P. J., and Petrini, J. H. (2001) Mre11 complex and DNA replication: linkage to E2F and sites of DNA synthesis, *Mol Cell Biol* 21, 6006-6016.
113. Lu, X., and Legerski, R. J. (2007) The Prp19/Pso4 core complex undergoes ubiquitylation and structural alterations in response to DNA damage, *Biochem Biophys Res Commun* 354, 968-974.

114. Bhalla, R. B., Schwartz, M. K., and Modak, M. J. (1977) Selective inhibition of terminal deoxynucleotidyl transferase (TdT) by adenosine ribonucleoside triphosphate (ATP) and its application in the detection of TdT in human leukemia, *Biochem Biophys Res Commun* 76, 1056-1061.
115. Kung, P. C., Siverstone, A. E., McCaffrey, R. P., and Baltimore, D. (1975) Murine terminal deoxynucleotidyl transferase: cellular distribution and response to cortisone, *J Exp Med* 141, 855-865.
116. Purugganan, M. M., Shah, S., Kearney, J. F., and Roth, D. B. (2001) Ku80 is required for addition of N nucleotides to V(D)J recombination junctions by terminal deoxynucleotidyl transferase, *Nucleic Acids Res* 29, 1638-1646.
117. Rea, S., Eisenhaber, F., O'Carroll, D., Strahl, B. D., Sun, Z. W., Schmid, M., Opravil, S., Mechtler, K., Ponting, C. P., Allis, C. D., and Jenuwein, T. (2000) Regulation of chromatin structure by site-specific histone H3 methyltransferases, *Nature* 406, 593-599.
118. Grillari, J., Ajuh, P., Stadler, G., Loscher, M., Voglauer, R., Ernst, W., Chusainow, J., Eisenhaber, F., Pokar, M., Fortschegger, K., Grey, M., Lamond, A. I., and Katinger, H. (2005) SNEV is an evolutionarily conserved splicing factor whose oligomerization is necessary for spliceosome assembly, *Nucleic Acids Res* 33, 6868-6883.
119. Loscher, M., Fortschegger, K., Ritter, G., Wostry, M., Voglauer, R., Schmid, J. A., Watters, S., Rivett, A. J., Ajuh, P., Lamond, A. I., Katinger, H., and Grillari, J. (2005) Interaction of U-box E3 ligase SNEV with PSMB4, the beta7 subunit of the 20 S proteasome, *Biochem J* 388, 593-603.

120. Ohi, M. D., Vander Kooi, C. W., Rosenberg, J. A., Chazin, W. J., and Gould, K. L. (2003) Structural insights into the U-box, a domain associated with multi-ubiquitination, *Nat Struct Biol* 10, 250-255.
121. Vander Kooi, C. W., Ohi, M. D., Rosenberg, J. A., Oldham, M. L., Newcomer, M. E., Gould, K. L., and Chazin, W. J. (2006) The Prp19 U-box crystal structure suggests a common dimeric architecture for a class of oligomeric E3 ubiquitin ligases, *Biochemistry* 45, 121-130.

CURRICULUM VITAE

Brian Douglas Beck

Education:

Butler University
Bachelor of Science, Chemistry; Biology
1998

Indiana University
Doctor of Philosophy, Biochemistry and Molecular Biology
2008

Honors, Awards, Fellowships:

Elise Turner Scholarship for Biological Sciences, Butler University, 1994-1998.
Butler Summer Institute Research Program, Butler University, 1997.

Research and Training Experience:

1999-2001 Examination of biochemical properties of the Mre11/Nbs1/Rad50 complex and Ku80 protein following heat shock and/or X-ray irradiation. Indiana University School of Medicine, Department of Biochemistry, Mentor: Dr. Joseph Dynlacht.

1997-1998 Purification of a 96-kD protein believed to be responsible for the adhesive properties of *Lottia limatula*, a coastal limpet. Butler University Department of Biological Sciences, Mentor: Dr. Andrew Smith.

Conferences Attended:

Midwest DNA Symposium, Lexington, Kentucky – 2003
Midwest DNA Symposium, Indianapolis, Indiana – 2006

Publications:

Dynlacht JR, Bittner ME, Bethel JA, Beck, BD. The Non-Homologous End-Joining Pathway Is Not Involved in the Radiosensitization of Mammalian Cells By Heat Shock. *J Cell Physiol.* 2003. 196(3): 557-64.

Beck BD, Dynlacht JR. Heat-Induced Aggregation of XRCC5 (Ku80) in Nontolerant and Thermotolerant Cells. *Radiat Res.* 2001. 156(6): 767-74.

Zhu WG, Seno JD, Beck BD, Dynlacht JR. Translocation of MRE11 From the Nucleus to the Cytoplasm as a Mechanism of Radiosensitization By Heat. *Radiat Res.* 2001. 156(1): 95-102.

Park SJ, Ciccone SL, Beck BD, Hwang B, Freie B, Clapp DW, Lee SH. Oxidative Stress/Damage Induces Multimerization and Interaction of Fanconi Anemia Proteins. *J Biol Chem.* 2004. 279(29): 30053-9.

Park SJ, Lee YJ, Beck BD, Lee SH. A Positive Involvement of RecQL4 in UV-Induced S-Phase Arrest. *DNA Cell Biol.* 2006. 25(12): 696-703.

Beck BD, Park SJ, Lee YJ, Roman Y, Hromas RA, Lee SH. Human Pso4 is a Metnase (SETMAR)-Binding Partner that Regulates Metnase Function in DNA Repair. *J Biol Chem.* 2008. 283(14): 9023-30.